ISSN 0376-7388, Journal of Membrane Science 524 (2017), pp. 321–333.

Experimental investigation and modeling through using the solution-diffusion concept of pervaporation dehydration of ethanol and isopropanol by ceramic membranes HybSi

Alexander V. Klinov [a], Roald R. Akberov [b, c, *], Azat R. Fazlyev [a, b], Mansur I. Farakhov [a, b]

[a] *Department of Chemical Engineering, Kazan National Research Technological University, 68 Karl Marx Str., Kazan, 420015, Russia*

[b] *LLC Engineering-Promotional Center "Inzhekhim", 14/83 Shalyapin Str., Kazan, 420049, Russia*

[c] *Research Laboratory "Perspective Systems of Orientation, Navigation and Communication" of the Institute of Physics, Kazan Federal University, 18 Kremlevskaya Str., Kazan 420008, Russia*

E-mail address: roaldakberov@yahoo.com (Roald R. Akberov)

Article history:
Received 15 July 2016
Received in revised form 16 November 2016
Accepted 17 November 2016
Available online 24 November 2016

Keywords: Pervaporation dehydration, HybSi membrane, Ethanol, Isopropanol, Solution-diffusion

DOI: 10.1016/j.memsci.2016.11.057

ABSTRACT

Results of experimental investigation of pervaporation dehydration of ethanol and isopropanol by HybSi membranes at concentrations of organic component in the feed in the range from ~50 to ~99 wt%, feed temperatures 60, 70 and 80°C and permeate pressures 5 and 20 mm Hg are presented. The experimental data demonstrate a nonmonotonic dependence of separation factor on water concentration in the feed with maximum value of separation factor reached at water concentration in the feed of several percent for both ethanol dehydration and isopropanol dehydration. Values of both total permeate flux and separation factor for the isopropanol dehydration case are higher than for the ethanol dehydration case. Results of the experimental investigation are compared with similar results of other researchers obtained for pervaporation dehydration of ethanol and isopropanol by membranes coated with a selective layer made of silica-based and zeolite-based materials. Based on the "solution-diffusion" concept, a mathematical model is developed for the pervaporation process, which includes three parameters, two of which are permeability coefficients for pure components and the third parameter defines "active pores fraction". Use of the model can lead to essential reduction of the number of pervaporation experiments needed for designing a pervaporation pilot plant as well as

assist in determining optimum operating conditions of the pervaporation process. Results of calculations carried out with use of the proposed model are compared versus results of experimental investigation of pervaporation dehydration of ethanol and isopropanol by HybSi membranes, pervaporation dehydration of glycerin by HybSi membranes (of other researchers) and pervaporation dehydration of ethanol by NaA zeolite-based membranes (of other researchers). Results of calculations agree reasonably well with all considered experimental data. Additionally, the model allows determining the optimum thickness of the selective layer of HybSi membranes.

1. Introduction

Ethanol and isopropanol are important organic solvents, which can be also used in industries for a great variety of other applications. When the two alcohols are used as additives for gasoline (for increasing octane number), antifreezes, deicing liquids, disinfectants, cosmetic products, solutions for offset printing and for some other purposes, absolute ethanol and isopropanol with residual concentration of water in the alcohols not exceeding a few tenths of a percent are required. However, due to formation of an azeotrope with water (for ethanol/water mixture: at concentration of alcohol ~96 wt%, and for isopropanol/water mixture: at concentration of alcohol ~88 wt% at atmospheric pressure), complete removal of water from the alcohols is impossible for conventional distillation; therefore, the distillation column undergoes changes involving either introduction of an azeotropic agent (e.g., benzene, phenol and cyclohexane) to the distillation column or generation of vacuum inside the column. In the former case, it is also required to remove the azeotropic agent from absolute alcohol afterwards to reduce alcohol's toxicity. As a rule, the distillation process is associated with large energy expenses.

As an alternative to conventional distillation processes, pervaporation technologies have been actively used in various industries during the last several decades. In line with data from the open literature [1], energy expenses for carrying pervaporation can be up to 60% lower than energy expenses for carrying out distillation for organic solvents dehydration. Despite the early discovery of the pervaporation phenomenon back at the turn of the 20th century, the first recorded industrial application of the technology took place only in 1982, when the GFT Company implemented its first ethanol dehydration pilot plants in Brazil (equipped with polymeric membranes coated with a selective layer made of polyvinyl alcohol) demonstrating the competitiveness of pervaporation versus azeotropic distillation. One of the latest and most perspective materials for the selective layer of asymmetric pervaporation membranes for dehydration applications is HybSi (which stands for "hybrid silica") developed at Energy Research Centre of the Netherlands (ECN) [2,3]. Hereinafter, tubular ceramic membranes coated with the selective layer made of HybSi will be referred to as HybSi membranes. During testing, HybSi membranes showed unprecedented thermal stability (up to 150°C during long-term operation and up to 190°C during short-term exposure) and chemical stability (2<pH<8) [2]. The longest test of HybSi membranes, which lasted three years, was accomplished at ECN on dehydration of n-butanol/water mixture (95/5 wt%) at temperature 150ºC [3]. For the duration of the test, separation factor of the membranes was virtually constant, though total permeate flux values somewhat decreased. In view of the superior characteristics, interest to HybSi membranes has been steadily growing [4–6].

In the present work, ethanol and isopropanol were chosen as alcohols for dehydration studies due to great industrial importance of the two alcohols, and tubular ceramic membranes coated on the inside with a selective layer made of HybSi (Pervatech BV, the Netherlands) were chosen as pervaporation membranes due to their superior characteristics. Measured dependences of total permeate flux and separation factor on concentration of water in the feed as well as some other dependences obtained in the present study can be potentially used for designing

pervaporation pilot plants equipped with HybSi membranes for industrial-scale dehydrating ethanol and isopropanol.

Due to necessity of carrying out a large number of pervaporation experiments for obtaining data needed for designing a pervaporation plant (at several values of feed temperature, permeate pressure, concentration of water in the feed and feed recirculation rate), a search for possibilities to replace a certain portion of experiments with calculated data is needed. In this regard, in the present work a mathematical model for describing the pervaporation process, which makes use of the "solution-diffusion" concept, is developed. The "solution-diffusion" approach was originally formulated in the 19th century for describing the process of passage of gases through caoutchouc films [7]. Later on, this approach was also applied to reverse osmosis, dialysis, vapor permeation and pervaporation. For the case of its application to pervaporation, there exist a number of published works, in which results of calculations carried out with use of the solution-diffusion model were compared versus experimental data [8–18]. Quite a reasonable agreement between the calculated and experimental data allows concluding regarding applicability of the "solution-diffusion" concept for modeling pervaporation. Due to this fact, in the present work, the "solution-diffusion" approach was used for describing pervaporation. During the model's development, a new parameter called "active pores fraction" was introduced. By using the parameter, it became possible to obtain a satisfactory agreement between calculated and experimental data. Results of calculations carried out with use of the developed model are compared versus our own experimental data on pervaporation dehydration of ethanol/water and isopropanol/water mixtures by HybSi membranes as well as versus experiments of other researchers on pervaporation dehydration of glycerin/water mixture by HybSi membranes [4] and pervaporation dehydration of ethanol/water mixture by membranes coated with the NaA zeolite [19]. The model allowed determining the optimum thickness of the selective layer of HybSi membranes. On the basis of results of the carried out investigation, conclusions can be drawn on applicability of the proposed model for assessing separation properties of already existing membranes from the minimum amount of experimental information.

2. Experimental

2.1. Ceramic membranes HybSi

A more detailed description of these membranes can be found in previous papers [2,3,5,6]. In brief, a material called HybSi for the selective layer of ceramic membranes was developed at ECN and represents an organic-inorganic hybrid material with an inorganic base; the organic fragments are sewed in the spatial structure of amorphous silica for increasing hydrothermal stability of the membranes. The inorganic part imparts hydrophilicity (wetting angle is ~70º) as well as mechanical strength, whereas the organic part imparts hydrothermal stability and enhanced viscosity so that propagation of nanocracks through the material decreases resulting in essential increase in the membrane's life in service. The membranes are thermally stable up to feed temperature ~150°C for long-term operation (and up to ~190°C for short-term exposure) and chemically stable at 2<pH<8 [2]. The longest test of HybSi membranes, which lasted three years, was accomplished at ECN on dehydration of n-butanol/water mixture (95/5 wt%) at temperature 150ºC. For the duration of the test, separation factor of the membranes remained virtually constant [3].

In this study, four tubular ceramic membranes HybSi (Pervatech BV, the Netherlands) were used with dimensions: length – 500 mm, inner diameter – 7 mm and outer diameter – 10 mm; total membrane surface area is 0.04 m^2. The tubes are coated on the inside with the HybSi material of thickness ~200 nm using the sol-gel technology with the pore size being no more than 1 nm. Between the selective layer and the ceramic support, there is an intermediate layer made of amorphous silica of thickness ~2000 nm with the pore size being approximately 4 nm. Arrangement of the tubes is in-series. A liquid feed flows inside the tubes and the permeating component vapor moves outwards to the space of the membrane module's shell under vacuum. It

is noteworthy that membranes used in the present study differ from membranes used in our previous studies [5,6]. Concerning the HybSi membranes used by other researchers for glycerin dehydration [4], it is known for certain that the membranes were purchased from the same membrane manufacturer (Pervatech BV, the Netherlands). Sizes, shapes, quantities and mutual arrangement of tubular HybSi membranes used in study [4] coincide with those used by us in our present study.

As to zeolite membranes from study [19], the researchers used one tubular membrane having dimensions: length – 400 mm, inner diameter – 5.8 mm and outer diameter – 7.3 mm. The selective layer, which is prepared by the secondary growth method from the NaA zeolite using seeds of diameter 0.15 μm, was applied on the outside of a porous (mean pore diameter is 0.12 μm) tube of α-Al_2O_3. Thickness of the selective layer is several micrometers. It should be noted that unlike the HybSi membranes used by us in the present study and by other researchers in study [4], the tubular membranes from [19] are coated with the selective layer on the outside instead of being coated on the inside. Thus, the feed mixture moves in an annular duct along the outer surface of the tube and vacuum is applied to inner space of the tube.

2.2. Experimental pervaporation unit

In view of the fact that the schematic of the experimental pervaporation unit used in the present study differs considerably from the schematic of the unit used by us in our previous studies [5,6], a detailed description of the new unit will be provided here. The schematic of the unit is shown in Fig. 1.

The unit consists of a feed (retentate) part and a vacuum (permeate) part. In the feed part, circulation of the feed between feed tank *1* and membrane module *3* takes place through lines *1* and *2* by means of vortex pump *2*. Pressure inside the closed loop is near atmospheric. The feed tank wall is equipped with a thermocable for maintaining a constant process temperature. Pervaporation takes place inside membrane module *3* containing four tubular ceramic membranes connected in series.

The feed moves inside a membrane tube with linear velocity of not less than 2 m/s, which is high enough for preserving concentration polarization at a low level. The permeate vapor leaves outwards to the intertubular space of the membrane module staying under vacuum created by vacuum pump of the membrane type *5*. The permeate vapor moves from membrane module *3* through line *3* and into shell-and-tube condenser *4*, where it cools and condenses. The cooling agent for the condenser is tap water. The non-condensed permeate vapor moves through line *4* and enters the flow-through cold traps *6*. The cooling agent for the cold traps, coming through line *5*, is ethanol at azeotropic concentration cooled by the KRIO-VT-05-02 cryostat *7* (LLC Termex, Russia).

The pipeline on line *5* as well as cold traps *6* are covered with a heat-insulating material for preventing heat losses to the environment. Material of the cold traps is stainless steel of grade AISI 304. The cold trap has the following dimensions: internal diameter – 45.3 mm, height – 370 mm, volume – 0.6 l.

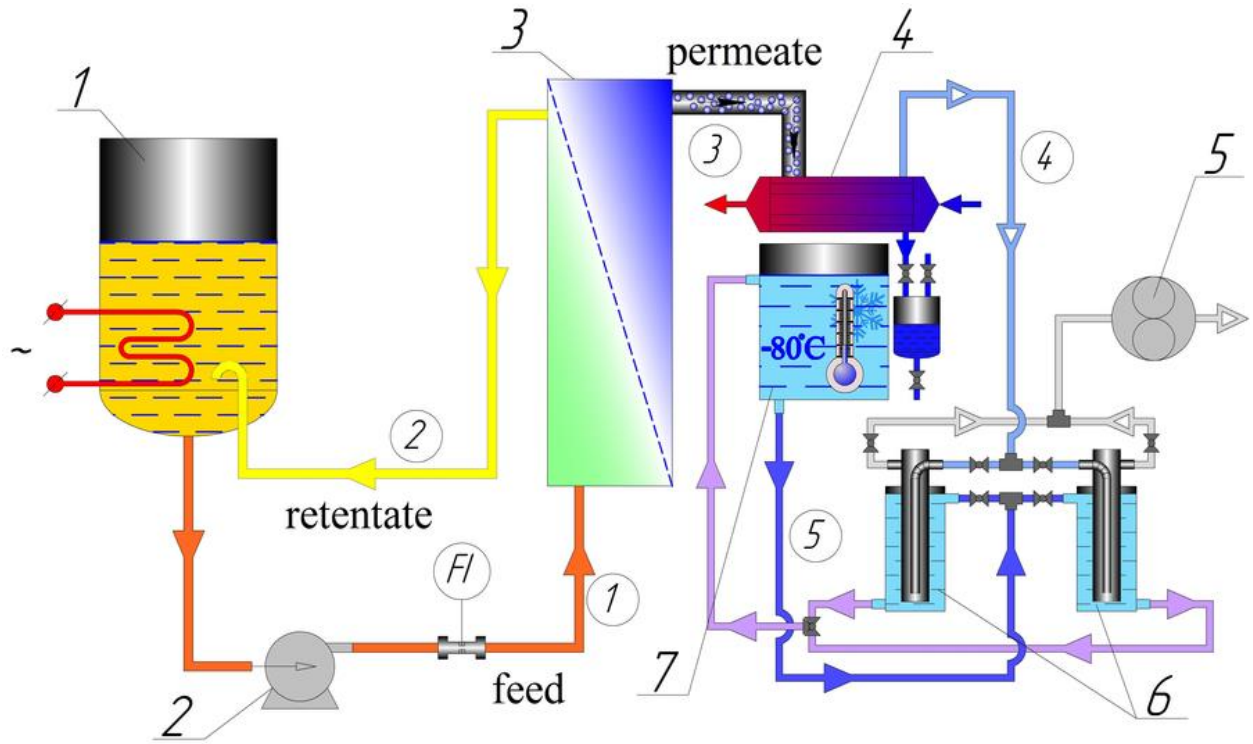

Fig. 1. Schematic of the experimental pervaporation unit: *1* – feed tank; *2* – feed pump; *3* – membrane module; *4* – condenser; *5* – vacuum pump; *6* – flow-through cold traps; *7* – cryostat.

2.3. Experimental procedures

Ethanol/water and isopropanol/water model mixtures are prepared from demineralized water (specific conductivity is 5 μS/cm) produced by the Osmodemi 12 unit (Idrotecnica s.r.I., Italy) and absolute ethanol or absolute isopropanol, in which the organic component has concentration not less than 99.8 wt%. The feed part of the unit is preliminarily purged with nitrogen to reduce oxygen concentration. Then the prepared feed mixture is poured to the feed tank *1*. Switching on the recirculation pump *2* and the feed tank's electric heater warms the feed to the desired temperature and forces it to circulate through the closed loop. Although the vacuum pump is still off at this time, a small portion of the feed permeates through the membrane pores and condenses on the permeate side of the membranes. Therefore, all the liquid collected at the bottom of membrane module *3* and inside the permeate collection vessel located under condenser *4* before the experiment begins are to be removed. After the vacuum pump is connected to the unit and the desired vacuum pressure is achieved in the permeate part of the unit, time reading begins. It takes less than 1 hour of unit operation to achieve adaptation of the membranes to feed temperature, feed composition and permeate pressure (which is also confirmed by studies [4,5] for pervaporation dehydration of organic solvents by HybSi membranes). Feed temperature in feed tank *1* and vacuum pressure in the intertubular space of membrane module *3* are kept constant during one experiment. A special attention is paid to the cooling agent's temperature for condensation of permeate vapor in condenser *4* and in flow-through cold traps *6*. The cooling agent for the condenser is tap water. When the permeate is collected using the combined scheme consisting of the condenser and the cold traps, condenser *4* lowers the permeate's temperature and captures a considerable portion of the permeate vapor. The remaining portion of the permeate vapor, which is not condensed, is trapped at temperature –80°C in flow-through cold traps *6* by phase transition of permeate from a vapor phase to a solid or liquid phase (in the present study, to a solid phase).

Removal of permeate, collected in flow-through cold traps *6*, is carried out as follows. Cold traps represent two stainless steel vessels, each of which is placed into a separate glass, through which the cooling agent flows. At one time, only one trap works while the second trap is

ready at call. Switching from one trap to the other is carried out manually, using the system of valves, whenever the operating trap is filled with permeate. Permeate collected inside a cold trap is molten (if it is in a solid phase) in periods between collectings of permeate. Then the permeate, taken out of the cold trap, is weighed on the AJ–1200CE scale (Shinko Denshi Co., Ltd., Japan) with accuracy ±0.01 g and added up to the permeate, taken out of condenser *4*, which is preliminarily weighed on the same scale. A small portion (a sample) of permeate is poored into a 2 ml vial and analyzed on gas chromatograph Crystal 2000M (ZAO Chromatec, Russia), preliminarily calibrated on ethanol/water and isopropanol/water mixtures of a known composition. After the permeate is removed, the cold trap is washed, dried, returns to a starting position and waits for its turn, while the second trap is operating. Collecting of permeate and of retentate samples is performed with intervals 15, 30 or 60 min depending on the amount of collected permeate. A sample of retentate is collected for analysis into a 2 ml vial through a sampler on line *2* and also analyzed on gas chromatograph Crystal 2000M for determining its chemical composition.

All pervaporation experiments are carried out at feed recirculation rate 350 l/h, which provides the turbulent regime of the feed's motion in the membrane tube of internal diameter 7 mm (mean velocity is 2.5 m/s, i.e. Re≈17000).

3. Modeling

In the HybSi membranes used in the present study (and in study [4]), the selective layer is applied on the inside of the tubes. Thus, the feed mixture (A+B) in the liquid phase, consisting of water (component A) and organic component (component B), moves inside a cylindrical membrane tube, and permeate is removed from the external surface of the tube in the vapor phase. It is assumed that influence of both a porous ceramic support made of α-Al_2O_3 and an intermediate layer made of amorphous silica on the pervaporation process can be neglected due to rather large pore sizes inside the two layers. In view of this fact, in this section the word "membrane" will be used only for a selective layer made of the HybSi material of thickness δ_m=~200 nm.

Depending on the membrane's selective properties, components A and B in a certain amount are transferred from an initial feed mixture through the membrane into the permeate zone. If the total permeate flux value and composition of permeate are known, the membrane's surface area F [m^2], required for the desired separation, can be easily calculated.

When the "solution-diffusion" concept is used (Fig. 2), the process of mass transfer of the initial feed mixture's components through the membrane into the permeate zone is split into the following stages: transfer from the retentate flow core to the membrane boundary, adsorption of components by the membrane's surface, diffusion of components through the membrane, desorption of components into the permeate region, transfer of components from the membrane boundary into the permeate stream. Let us consider these stages of mass transfer separately, i.e. step by step.

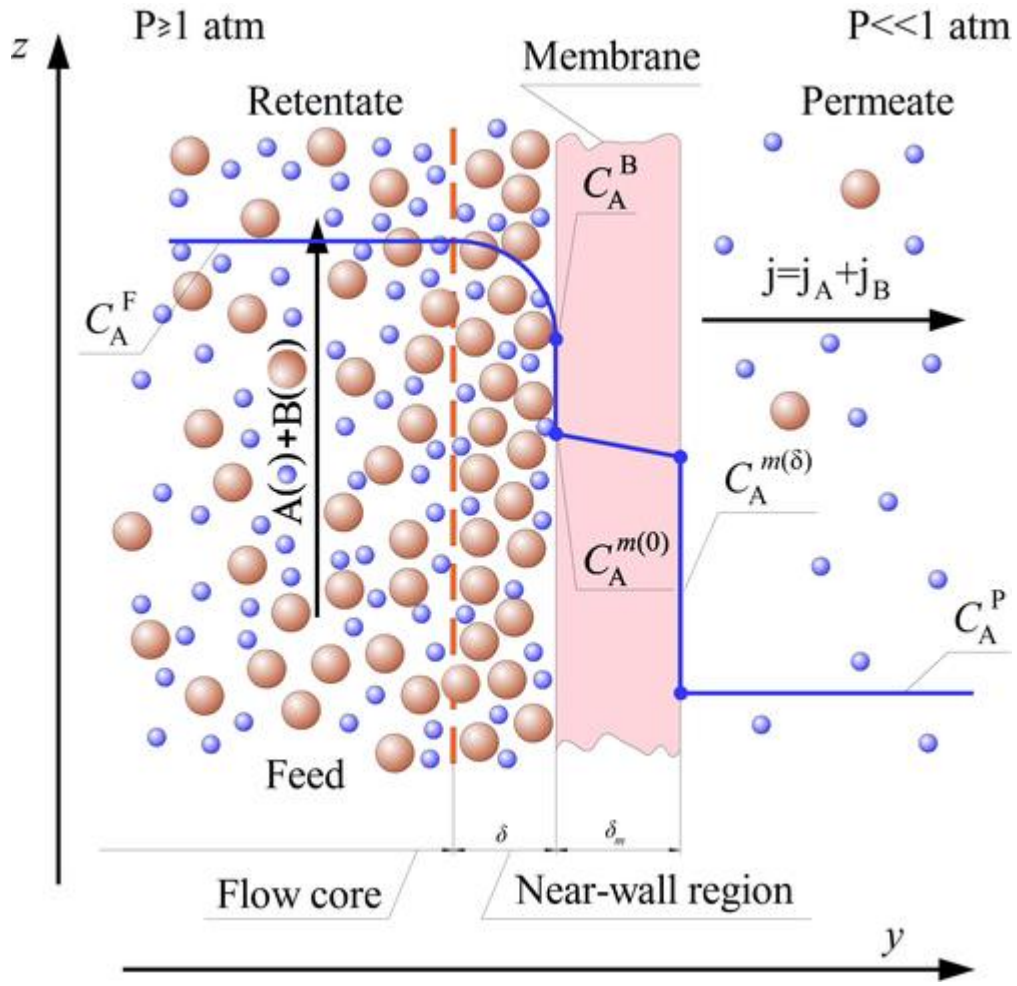

Fig. 2. Theoretical model of pervaporation of a binary mixture through a dense (non-porous) membrane (i.e. through a selective layer of the membrane) based on the "solution-diffusion" concept. Components: A – water; B – organic matter.

When the feed mixture moves in the turbulent regime, the retentate (feed) zone is comprised of two distinct regions: flow core and near-wall region. In the flow core, the profile of concentration of components in the transverse direction (in y-axis direction), due to intensive turbulent exchange, can be considered as uniform. The main changes of fluid flow velocity and of concentration of mixture components in the transverse direction take place across the near-wall region. Therefore, main resistance to mass transfer is concentrated in the near-wall region, and mass transfer is carried out by the following three main mechanisms: molecular, turbulent and convective mechanisms. The molar reference system for determining diffusion rates gives the following expression for the molar flux of component A, j_A:

$$j_A = -(D_{AB} + D_{AB}^T)\, C \frac{dx_A}{dz} + j x_A, \qquad (1)$$

where j_A is molar flux of component A through the membrane [mole/(m^{2}s)]; j is total molar flux of two components through the membrane [mole/(m^{2}s)]; D_{AB} is mutual diffusion coefficient in the molar reference system [m^2/s]; D_{AB}^T is turbulent diffusion coefficient [m^2/s]; x_A is mole fraction of component A; C is molar density of the mixture [mole/m^3].

Integrating expression (1) through the near-wall region having thickness δ gives:

$$\frac{x_A^F\, j - j_A}{x_A^B\, j - j_A} = \exp\left(- j \int_0^{\delta} \frac{dy}{(D_{AB} + D_{AB}^T) C} \right).$$

Here x_A^B is mole fraction of component A in the solution on the membrane boundary.

The integral on the right-hand side can be set equal to the inverse of mass transfer coefficient β^0, [m/s], as a first approximation, if no convective flux is assumed to take place through the near-wall region:

$$\int_0^{\delta} \frac{dy}{(D_{AB} + D_{AB}^T)C} \approx \frac{1}{\beta^0}, \qquad (2)$$

where β^0 is mass transfer coefficient for the "no-convective flux" case [m/s].

Strictly speaking, expression (2) will hold true for the wall film model, if the condition $D_{AB}C = const$ is fulfilled or relative diffusion flux of component A across the near-wall region is maintained constant [20].

$$\frac{x_A^F j - j_A}{x_A^B j - j_A} = \exp(-j/\beta^0).$$

If transverse convective flux is present, mass transfer coefficient is defined as:

$$\beta = \frac{j_A - x_A^B j}{x_A^F - x_A^B},$$

and a final expression for flux of component A from the flow core to the membrane surface is written as:

$$j_A = \beta (x_A^F - x_A^B) + j x_A^B, \qquad (3)$$

where $\beta = j/[1 - \exp(-j/\beta^0)]$; β is defined in [mole/(m^{2}s)].

An expression for flux of component B can be obtained from expression (3) by substitution: $x_A = 1 - x_B$.

Stages of components adsorption by the membrane, mass transfer through the membrane and components desorption can be considered jointly. We will adopt the assumption of zero convective flux through the membrane and main assumptions of the "solution-diffusion" model of adsorption equilibrium reaching on membrane boundaries as well as constant pressure across the membrane. The following expression for flux of component A through the membrane can be obtained as [21]:

$$j_A = D_A^m K_{1A} \frac{(p_A^B K_{2A} - p_A^P)}{\delta_m}. \qquad (4)$$

Here D_A^m is diffusion coefficient of component A in the membrane [m^2/s]; p_A^B and p_A^P are values of partial pressure of component A on the boundary with the membrane in the solution and in permeate, respectively [Pa]; $K_{1A} = \frac{C^{m(\delta)}}{p_A^S \gamma_A^{m(\delta)}}$, $K_{2A} = \frac{C^{m(0)} \gamma_A^{m(\delta)}}{C^{m(\delta)} \gamma_A^{m(0)}}$. $\gamma_A^{m(0)}$ and $\gamma_A^{m(\delta)}$ are activity coefficients of component A on the inside of the membrane on the membrane boundaries; $C^{m(0)}$ and $C^{m(\delta)}$ are total molar density of the substance on the inside of the membrane on the membrane boundaries [mole/m^3]; p_A^S is saturated vapor pressure of component A [Pa]. Because of difficulty to determine values of coefficients K_{1A} and K_{2A}, expression (4) can be rewritten for practical purposes as follows:

$$j_A = P_A^m \frac{(p_A^B - p_A^P)}{\delta_m}. \qquad (5)$$

Here P_A^m is permeability coefficient of component A [mole/(m·s·Pa)]. Note that coefficient K_{2A} accounts for non-uniform distribution of a substance across the membrane. Therefore, in case of

high non-uniformity and of its influence on the substance's flux, coefficient K_{2A} should be preserved in equation (5) as a parameter of the model.

Partial pressure of component A in the solution on the membrane boundary can be written as: $p_A^B = p_A^S \gamma_A^B x_A^B$, where γ_A^B is activity coefficient of component A in the liquid phase on the membrane boundary. An expression for partial pressure in permeate can be written as: $p_A^P = p^P x_A^P$, where p^P is permeate pressure [Pa]; x_A^P is mole fraction of component A in permeate. An expression for flux of component A through the membrane, j_B [mole/(m^2s)], can be written analogously to equation (5) as:

$$j_B = P_B^m \frac{(p_B^B - p_B^P)}{\delta_m}. \qquad (6)$$

Here P_B^m is permeability coefficient of component B [mole/(m·s·Pa)]; p_B^B and p_B^P are values of partial pressure of component B on the membrane boundaries in the solution and in permeate, respectively [Pa].

As for the last stage, i.e. transfer of a substance from the membrane boundary to the permeate stream, one can avoid considering it at all, if concentration of components in permeate on the membrane boundary is taken equal to concentration of components inside the permeate stream, which is true, as mass transfer from the membrane boundary to the permeate stream occurs by convective flux directed normally from the membrane surface.

If the pervaporation process is conducted under steady-state conditions, the amount of a substance transferred from the flow core to the membrane surface is equal to the amount of a substance transferred through the membrane. It is important to note the following. In ceramic membranes HybSi, mass transfer through the selective layer is not carried out through the entire surface area (as in polymeric membranes, for example). Instead, a substance is transferred through channels in the selective layer, and the amount of a substance transferred through the membrane per unit time can be written as: $N_A = j_A F \varepsilon$, where F is the selective layer's surface area [m^2]; ε is fraction of channels, whose sizes permit molecules of the feed mixture passing through. A permoporometric study of HybSi membranes revealed that the channels have diameters not exceeding 10 Å [3]. During mass transfer, molecules of the feed mixture are adsorbed on the membrane surface, including adsorption on the channels, but, due to differencies in sizes of molecules and in energies of their interaction with the membrane surface, they tend to vacate the channels at different rates when penetrating the membrane. Therefore, it can be assumed that not all channels are available (i.e. active) for moleclues of the feed mixture to pass through, since a certain fraction of channels turns out to be blocked by adsorbed molecules. If one describes a fraction of occupied channels via an expression similar to Langmuir's adsorption isotherm:

$$\varepsilon_{oc} = \frac{C_{pA} + C_{pB}}{C_p} = \frac{C_A k_A + C_B k_B}{1 + C_A k_A + C_B k_B},$$

then active pores fraction (or active channels fraction) can be written as:

$$\varepsilon_a = 1 - \varepsilon_{oc} = \frac{1}{1 + C_A k_A + C_B k_B}.$$

In these expressions, C_p is total number of channels per unit volume; C_{pA} and C_{pB} are values of number of channels occupied by components A and B, respectively; C_A and C_B are values of volumetric-molar concentration of components A and B in the solution on the membrane boundary; k_A and k_B are dimensionless coefficients having a meaning similar to chemical reaction rate constants. For example, $k_A = k_{A1}/k_{A2}$, where k_{A1} is adsorption rate of component A on the channels, and k_{A2} is desorption rate, which represents a sum of desorption rates of a component into the solution and into the membrane. If the membrane is selective with

respect to component A, then, as a good approximation, one can adopt that $k_A << k_B$. Then a final expression for active pores fraction will take the form:

$$\varepsilon_a = \frac{1}{1 + C_B k_B} = \frac{1}{1 + C x_B k_B}. \quad (7)$$

As a result, the following system of equations can be obtained for steady-state conditions:

$$\beta (x_A^F - x_A^B) + j x_A^B = P_A^m \frac{(p_A^B - p_A^P)}{\delta_m} \varepsilon_a, \quad (8)$$

$$\beta (x_A^B - x_A^F) + j(1 - x_A^B) = P_B^m \frac{(p_B^B - p_B^P)}{\delta_m} \varepsilon_a. \quad (9)$$

In addition, taking into account a connection between permeate's composition and component fluxes, one more equation is added to the system:

$$x_A^P = \frac{j_A}{j} = \frac{\beta (x_A^F - x_A^B) + j x_A^B}{j} \quad (10)$$

The obtained system (8)–(10) allows determining three unknown parameters. For example, if the following process conditions are known: feed temperature T, permeate pressure p^P, composition of the initial feed mixture as well as geometry of the membrane module and the plant's capacity (for determining β^0), then the solution to the system (8)–(10) will be composition of the liquid mixture on the boundary retentate-membrane (x_A^B), composition of permeate (x_A^P) as well as total molar flux j, which can easily be transformed to the total mass flux $\bar{j}$. Next, it is easy to determine mass fluxes of both components, $\bar{j}_A$ and $\bar{j}_B$, and separation factor with respect to component A, α. Thus, the mathematical model in the form of the system (8)–(10) accounts for influence of all main factors on the pervaporation process and allows determining the process characteristics in the form of component fluxes and permeate's composition required for calculating and designing membrane modules.

Activity coefficients of components in the liquid phase were determined by the NRTL model [22]. Mass transfer coefficient β^0 was calculated from Sherwood number, Sh: $\beta^0 = D_{AB} Sh / d_{in}$ using the assumption of a fully-developed turbulent flow in a cylindrical tube in the absence of any phase transitions via the following criterion equation [23]:

$$Sh = 0.021 Re^{0.8} Sc^{0.43} \quad (11)$$

where $Re = d_{in} w_{lin} / \nu$ is Reynolds number; $Sc = \nu / D_{AB}$ is Schmidt number; ν is kinematic viscosity of liquid [m^2/s]; w_{lin} is mean velocity of liquid in the tube [m/s] , d_{in} is internal diameter of the membrane tube [m].

The mathematical model (8)–(10) contains three parameters determined from experiments: permeability coefficients P_A^m and P_B^m for pure components A and B, respectively, and parameter k_B, which defines dependence of active pores fraction on composition of the solution on the membrane boundary. Permeability coefficient of water, P_A^m, was determined independently using experimental data for pure water pervaporation. Permeability coefficient of an organic component, P_B^m, and parameter k_B were calculated using a value of organic component flux for the feed mixture containing ~0.01 mol% water and one or two values of water flux for the feed mixture containing 30–70 mol% water. In the first case, one can neglect presence of water in the mixture and consider only equation (9). In the second case, in this concentration region, influence of active pores fraction starts being essential, and, at the same time, organic component flux through the membrane turns out to be much smaller than water flux, which allows adopting that $j = j_A$, $j_B = 0$ and $x_A^P = 1$. Simultaneous solution of equations (8)–(10) using the adopted simplifications gives values of parameters P_B^m and k_B.

Table 1. Measured values of pure water flux and pure organic component flux through HybSi and NaA-zeolite membranes for various feed temperatures, permeability coefficients calculated via using the measured fluxes and linear approximation for temperature dependencies of the fluxes.

Component		Flux of pure component, kg/(m^{2}h) // Permeability coefficient ·10^{11}, kg/(m·h·Pa)			Coefficients of linear approximation for fluxes: $(C_1T^* + C_2)$	
		60°C	70°C	80°C	C_1	C_2
Water	HybSi	6.46 // 7.426	9.15 // 6.445	12.01 // 5.353	0.2775	–10.2183
	NaA	–	2.66 // 1.283	–	–	–
Ethanol	HybSi	0.08 // 0.095	0.12 // 0.085	0.16 // 0.072	0.0039	–0.1513
	NaA	0 // 0	0 // 0	0 // 0	–	–
Isopropanol	HybSi	0.017 // 0.0013	0.011 // 0.0036	0.02 // 0.0041	0.0008	–0.0457
Glycerin	HybSi	0 // 0	0 // 0	0 // 0	–	–

For pervaporation dehydration of ethanol and isopropanol by HybSi membranes, there exist all the data required for determining dependences of the above model parameters on feed temperature. Table 1 presents measured values of pure water flux and pure organic component flux through HybSi and NaA-zeolite membranes as well as permeability coefficients (in units [kg/(m·h·Pa)] obtained from [mole/(m·s·Pa)] through molecular weight) calculated via measured flux values. Results of our experiments and experiments from [4,19] have shown that dependence of pure component fluxes on feed temperature in the temperature range T^*=60–80°C has a linear character: $(C_1T^* + C_2)$, where T^* is feed temperature in degrees Celsius; C_1 and C_2 are coefficients of linear decomposition, whose values are presented in Table 1. For glycerin dehydration by HybSi membranes, the value of glycerin flux equals zero as HybSi membranes turned out to be practically impermeable for glycerin [4]. For exactly the same reason, ethanol flux value through the NaA-zeolite membranes is specified as being zero in Table 1. For dehydration of ethanol and isopropanol by HybSi membranes, permeate pressure was equal to 20 mm Hg, and for dehydration of glycerin, permeate pressure was equal to 7.5 mm Hg. For dehydration of ethanol by NaA-zeolite membranes, permeate pressure was equal to 1 mm Hg. Behavior of parameter k_B is approximated quite well by an equation having an appearance of the Arrhenius equation: $k_B = A\exp(-E/T)$. Coefficients A and E of this approximation have the same meaning as coefficients in the standard Arrhenius equation, i.e. A is pre-exponential factor; E is activation energy for pervaporation. It turns out that cases of ethanol dehydration and isopropanol dehydration by HybSi membranes possess the same dependence $k_B(T)$: A=8.078·10^{-9} m^3/mole, E=5446.374 K. With increase in feed temperature, value of parameter k_B decreases due to increase in permeation rate of an organic component into the membrane. Experimental data for glycerin dehydration by HybSi membranes from [4] and for ethanol dehydration by zeolite membranes from [19] are available only for one value of feed temperature not allowing determining temperature dependences of the proposed model parameters.

4. Results and discussion

4.1. Dependence of concentration of an organic component in the feed on time for dehydrating ethanol and isopropanol by HybSi membranes

Pervaporation dehydration of ethanol and isopropanol by HybSi membranes was carried out in the range of organic component concentration in the feed from ~50 wt% to ~99 wt%. Feed temperature was taken equal to 60, 70 and 80°C and permeate pressure was taken equal to 5 and 20 mm Hg for ethanol dehydration and 20 mm Hg for isopropanol dehydration. Initial weight of feed was ~2.6 kg and feed recirculation rate was 350 l/h.

Figure 3 presents dependencies of organic component concentration in the feed on time. The horizontal dashed line corresponds to concentration 97 wt%, achieved in all experiments of the present study.

Water concentration in the feed decreases with time for both binary systems meaning that HybSi membranes are selective to water. Permeate pressure decrease from 20 to 5 mm Hg in the ethanol dehydration case leads to increase in the driving force of the process. It is noteworthy that the curves, corresponding to ethanol dehydration at permeate pressure 5 mm Hg, closely coincide with the curves, corresponding to isopropanol dehydration at permeate pressure 20 mm Hg. Hence, the required membrane surface area for these two separation tasks will be very similar [6].

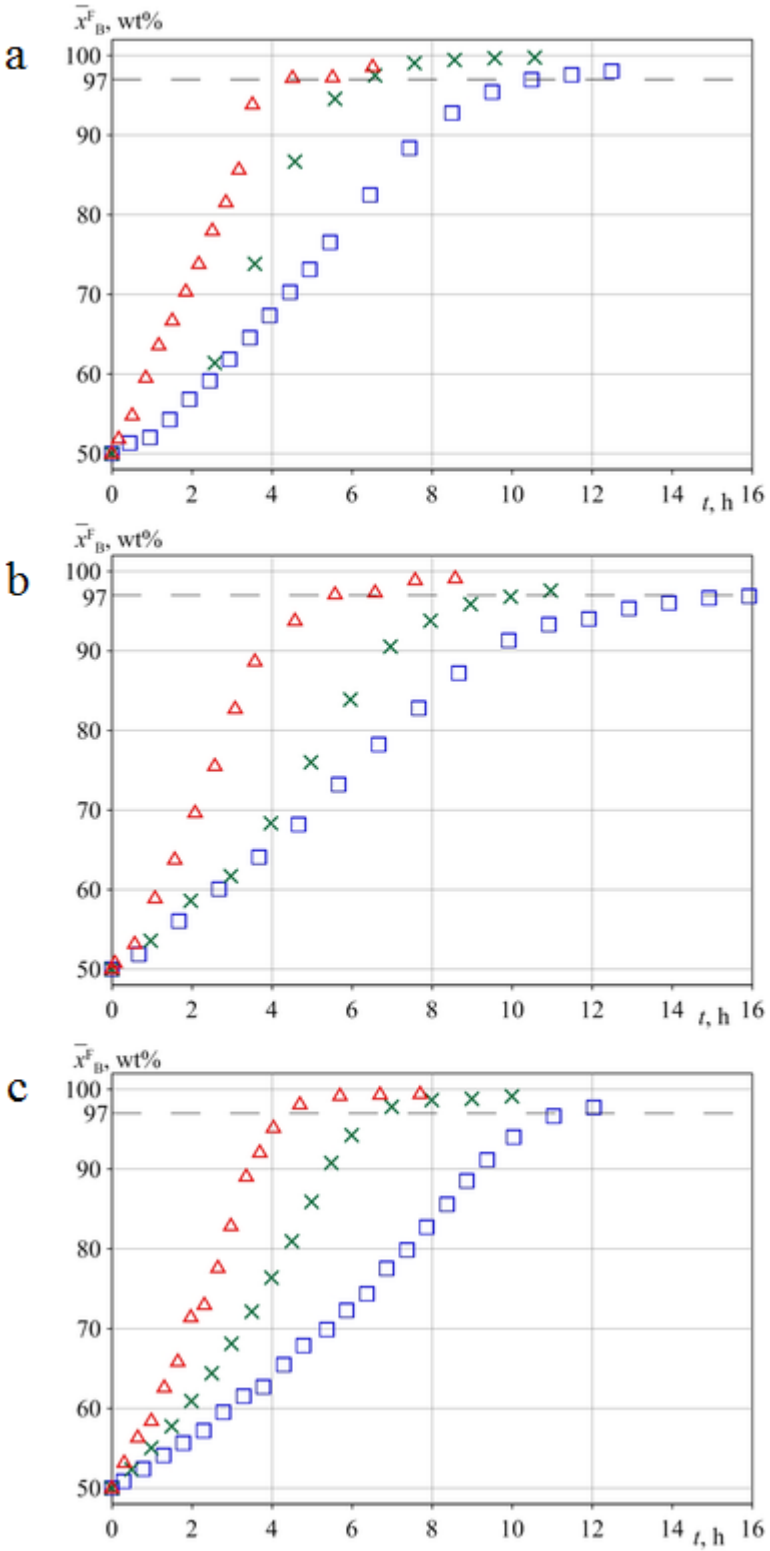

Fig. 3. Dependence of organic component concentration in the feed on time for dehydration in the range from ~50 to ~99 wt% at feed temperature 60°C (blue squares), 70°C (green crosses) and 80°C (red triangles) by HybSi membranes of total surface area 0.04 m^2 for initial feed's weight ~2.6 kg at feed recirculation rate 350 l/h. (a) dehydration of ethanol at permeate pressure 5 mm Hg; (b) dehydration of ethanol at permeate pressure 20 mm Hg; (c) dehydration of isopropanol at permeate pressure 20 mm Hg.

4.2. Dependence of permeate fluxes on water concentration in the feed for dehydrating ethanol and isopropanol by HybSi membranes

Values of total permeate flux $\bar{j}$ [kg/(m^{2}h)] and separation factor α were determined from measured data using the following expressions:

$$\bar{j} = \frac{m^P}{F\,\Delta t}, \tag{12}$$

$$\alpha = \frac{\bar{x}_A^P / \bar{x}_A^F}{\bar{x}_B^P / \bar{x}_B^F}, \tag{13}$$

where m^P is weight of permeate [kg] collected within sampling time Δt [h], F is membrane surface area [m^2], $\bar{x}_A^P$ and $\bar{x}_B^P$ are mass concentrations of components A and B in permeate, respectively [wt%], $\bar{x}_A^F$ and $\bar{x}_B^F$ are mass concentrations of components A and B in retentate (i.e. in the feed), respectively [wt%]. Fluxes $\bar{j}_A$ and $\bar{j}_B$ of components A and B, respectively, were determined using the following expressions: $\bar{j}_A = \bar{j}\bar{x}_A^P$; $\bar{j}_B = \bar{j}\bar{x}_B^P$.

Figures 4, 5 and 6 show measured values of water flux $\bar{j}_A$, organic component flux $\bar{j}_B$ and total permeate flux $\bar{j}$, respectively. Values of separation factor α are not presented here, as they can be easily obtained from Fig. 4, 5 and 6. As is seen from Fig. 4, the values of water flux through HybSi membranes are higher for isopropanol/water mixture dehydration than for ethanol/water mixture dehydration for a wide concentration range in identical process conditions. On the other hand, it follows from Fig. 5 that, for identical process conditions, the greater value of organic component flux is observed for ethanol dehydration, which is greater by one order of magnitude than that for isopropanol dehydration. The differences in permeation of an organic component through HybSi membranes can be attributed to differences in sizes of molecules of ethanol and isopropanol, which can lead to differences in diffusion of the substances through the membranes (an ethanol molecule is smaller than an isopropanol molecule). In addition, if one compares relative volatility of water in the considered mixtures, then relative volatility increases in the order: ethanol/water, isopropanol/water, which can serve as an additional explanation for differences in permeation of the two organic substances through the membranes. From Fig. 4, 5 and 6 it follows that permeate pressure exerts influence on the permeate flux values.

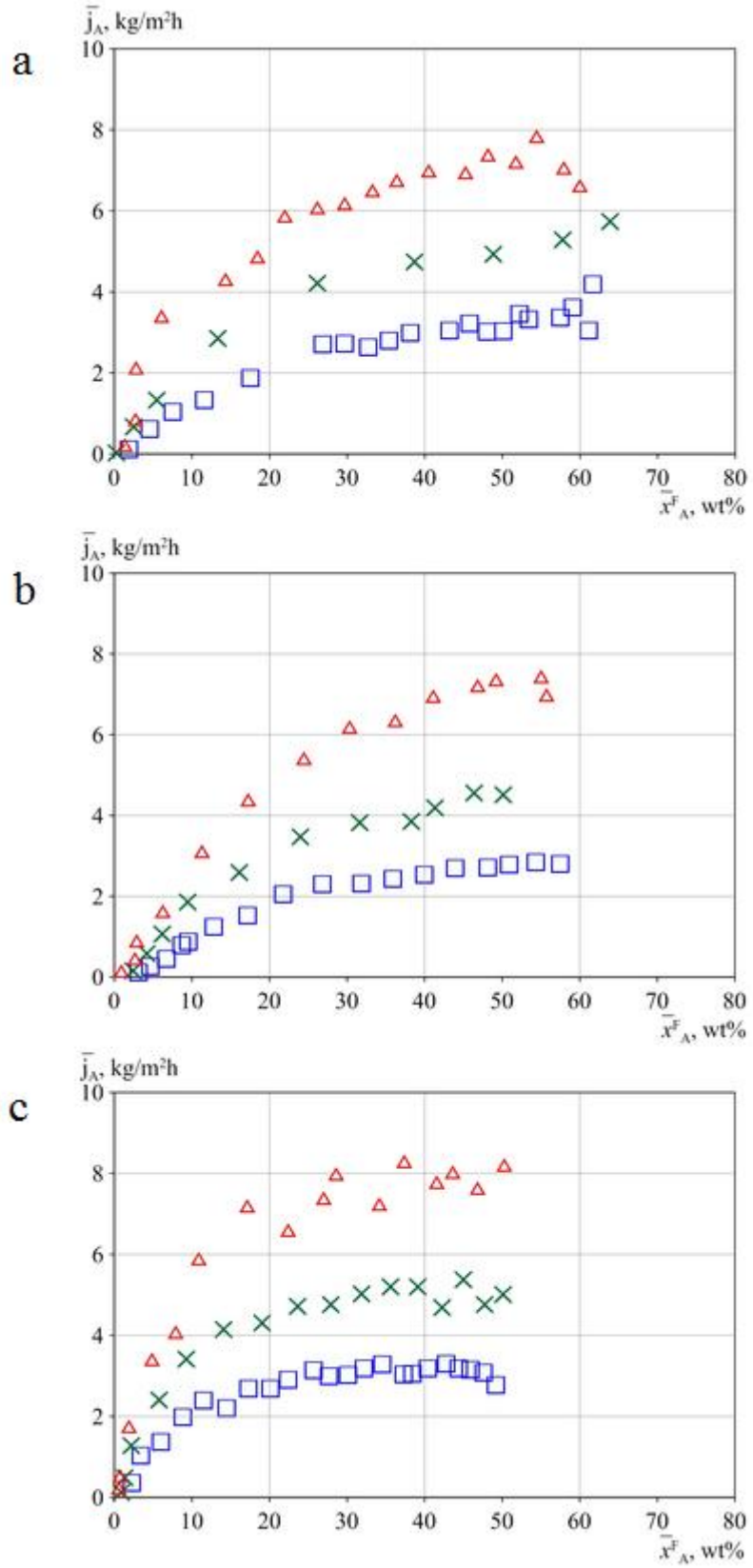

Fig. 4. Dependence of water flux through HybSi membranes on water concentration in the feed at feed temperature 60°C (blue squares), 70°C (green crosses) and 80°C (red triangles). (a) dehydration of ethanol at permeate pressure 5 mm Hg; (b) dehydration of ethanol at permeate pressure 20 mm Hg; (c) dehydration of isopropanol at permeate pressure 20 mm Hg.

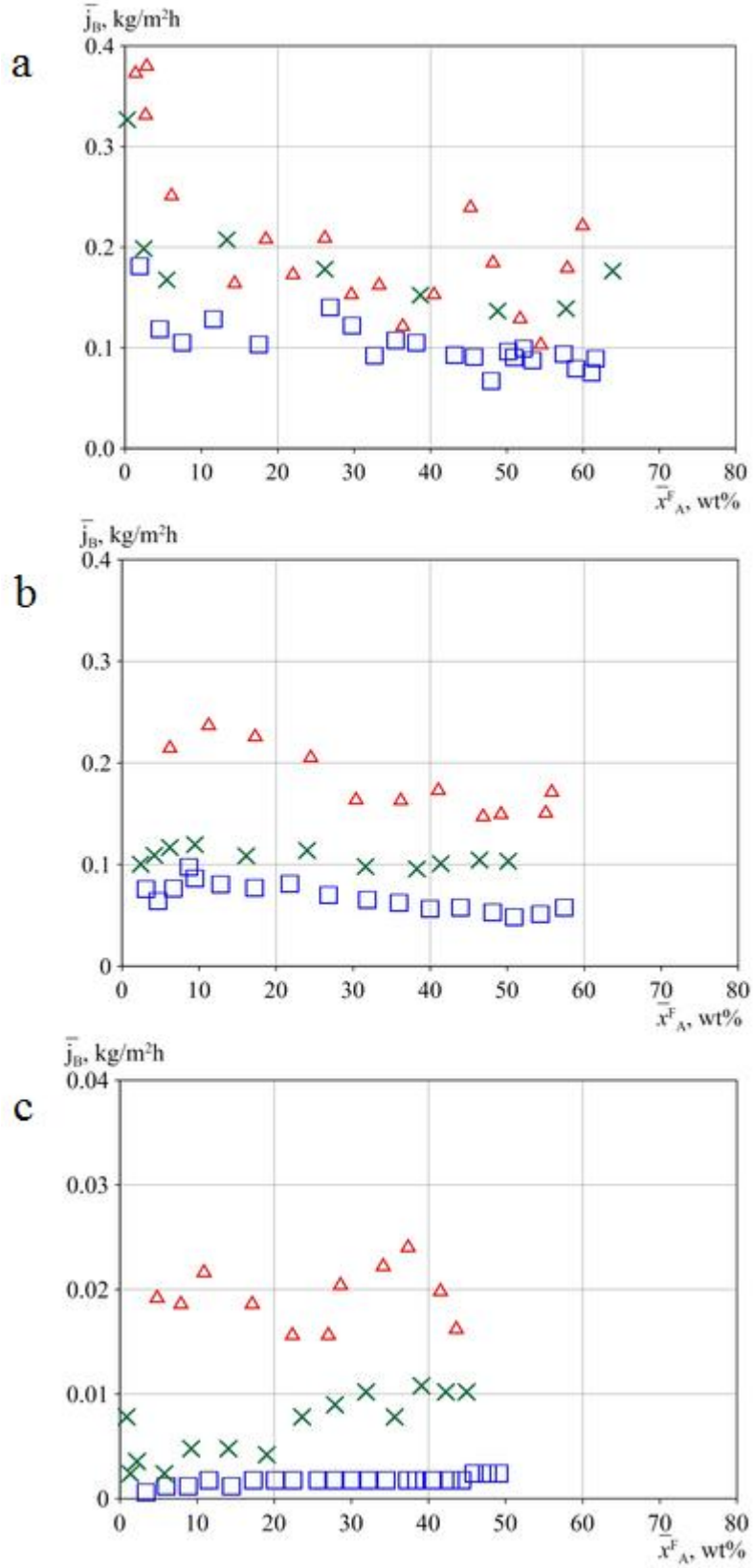

Fig. 5. Dependence of organic component flux through HybSi membranes on water concentration in the feed at feed temperature 60°C (blue squares), 70°C (green crosses) and 80°C (red triangles). (a) dehydration of ethanol at permeate pressure 5 mm Hg; (b) dehydration of ethanol at permeate pressure 20 mm Hg; (c) dehydration of isopropanol at permeate pressure 20 mm Hg.

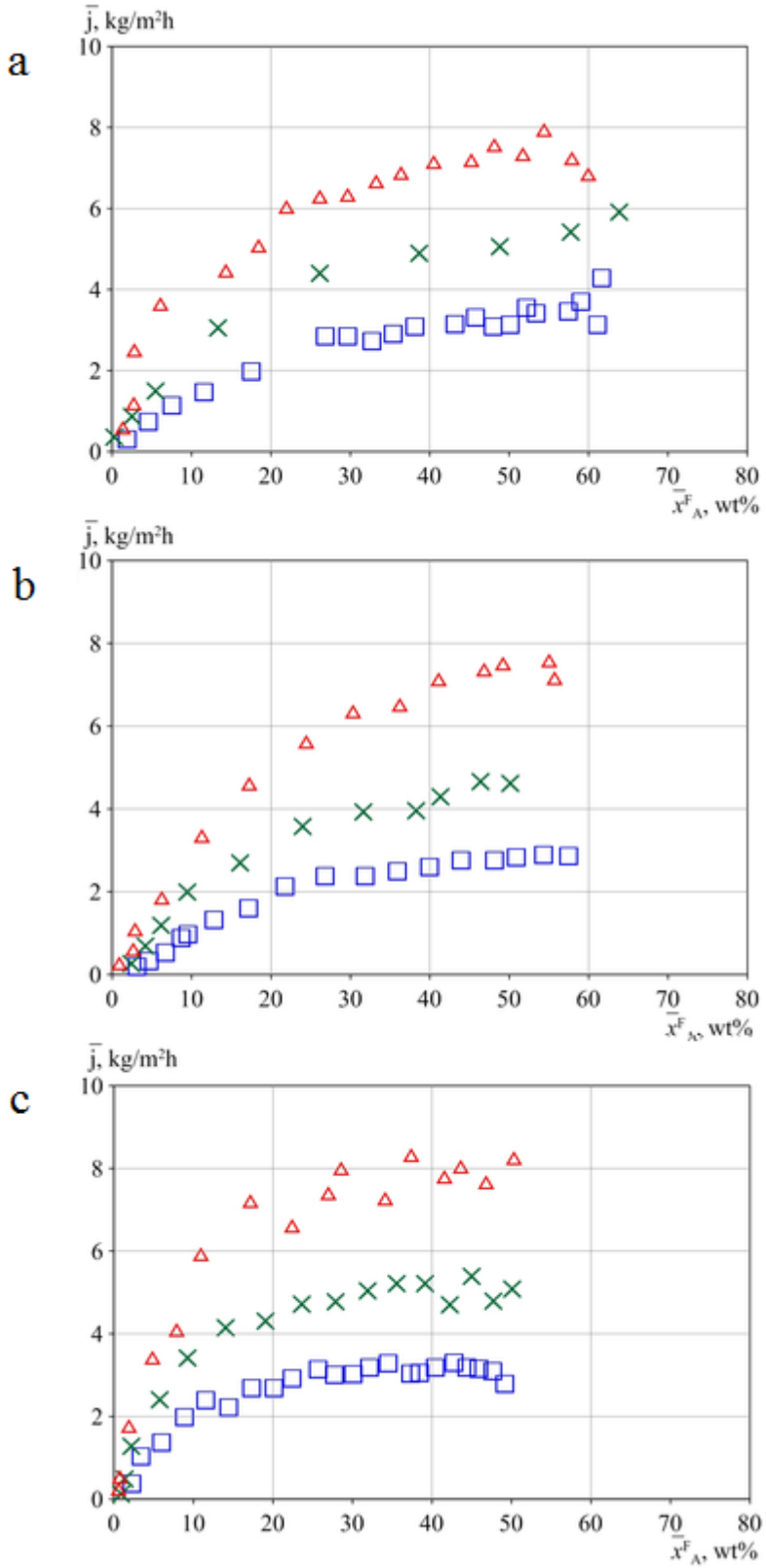

Fig. 6. Dependence of total permeate flux through HybSi membranes on water concentration in the feed at feed temperature 60°C (blue squares), 70°C (green crosses) and 80°C (red triangles). (a) dehydration of ethanol at permeate pressure 5 mm Hg; (b) dehydration of ethanol at permeate pressure 20 mm Hg; (c) dehydration of isopropanol at permeate pressure 20 mm Hg.

4.3. Comparing our experimental data versus experimental data of other researchers

Pervaporation dehydration of ethanol and isopropanol has been studied intensively in laboratories during the last several decades by using membranes made of various materials, including polymer, chitosan, zeolite, silica, zirconia, titania and other materials, and various shapes, including flat sheet, spiral-wound, hollow-fiber and tubular shapes. We selected a limited number of relatively modern publications devoted to investigation of dehydration of ethanol and isopropanol by pervaporation membranes of a tubular shape having a selective layer made of silica or NaA zeolite.

Table 2 presents a comparison of our experimental data with data from the literature on pervaporation dehydration of ethanol and isopropanol at water concentration in the feed 5 wt% obtained under similar process conditions. Feed temperature in all these datasets was 70–80ºC, but permeate pressure values varied from one dataset to another in a rather wide range. Permeate pressure can exert a certain influence on total permeate flux $\bar{j}$ and separation factor α, though not so essential as feed temperature inside the membrane module [5].

Table 2. Comparison of our experimental data with literature data for pervaporation dehydration of ethanol and isopropanol by tubular silica and NaA zeolite membranes for the case of water concentration in the feed 5 wt%.

Organic matter	Material of selective layer	Selective layer is coated	Feed, ºC	Permeate pressure, mm Hg	$\bar{j}$, kg/(m²h)	α	Ref.
Ethanol							
	Silica	Outside	70	3.8	1.350	200	[24]
	Silica	Outside	70	≤1.5	0.200	100	[25]
	NaA zeolite	Outside	75	13.5	1.100	5900	[26]
	NaA zeolite	Outside	70	≤1.0	0.029	>10000	[19]
	HybSi	Inside	80	20.0	1.500	120	Present study
Iso-propanol							
	Silica/zirconia (50/50)	Outside	75	≤6.0	2.050	800	[27]
	Silica	Outside	80	19.0	1.900	1200	[24]
	Silica	Outside	70	≤1.5	0.250	500	[25]
	Silica	Outside	70	≤0.8	2.100	600	[28]
	NaA zeolite	Outside	70	5.0	0.230	2000	[29]
	HybSi	Inside	80	20.0	3.380	10000	Present study

Note: Some of the values of $\bar{j}$ and α in the table are not exact values, since they were obtained by interpolation (or extrapolation) to organic component concentration in the feed 95 wt% or calculated from other data presented in the cited publications.

As is seen from the data for isopropanol dehydration, under similar process conditions, HybSi membranes outperform all the remaining membranes from the table in both total permeate flux $\bar{j}$ and separation factor α. In addition, it can be found that, for isopropanol dehydration, HybSi membranes have values of both $\bar{j}$ and α considerably higher than the values for ethanol dehydration under identical conditions. This observation compares well with observation for the case of dehydrating ethanol and isopropanol by conventional silica membranes [24]. Lower

values of α for silica-based membranes, when used for ethanol dehydration, can be best explained by a rather large mean size of pores in amorphous silica (~1 nm) and similar sizes of molecules of water and ethanol (both a water molecule and an ethanol molecule can pass through the pores).

The table shows that, when HybSi membranes are used for isopropanol dehydration, values of $\bar{j}$ and α turn out to be comparable to those corresponding to isopropanol dehydration by the other membranes. In addition it can be found that various zeolite and silica membranes possess values of $\bar{j}$ and α differing from each other by not more than one order of magnitude. For ethanol dehydration by HybSi membranes, values of α are close to those corresponding to ethanol dehydration by the other silica-based membranes, whereas values of $\bar{j}$ differ from each other, but the differences are within one order of magnitude.

In contrast to ethanol dehydration by silica-based membranes, at dehydrating ethanol by NaA zeolite-based membranes, values of α make around several thousand, meaning that the membranes are practically impermeable to ethanol, whereas values of $\bar{j}$ can be both lower and higher than those corresponding to ethanol dehydration by silica-based membranes.

4.4. Comparing calculated and measured dependencies of water flux through HybSi membranes on water concentration in the feed for dehydrating ethanol and isopropanol

Figure 7 presents measured and calculated values of water flux through HybSi membranes depending on water concentration in the feed for dehydrating ethanol and isopropanol. In addition to experimental points of Fig. 4, a supplementary experimental point on the right, corresponding to pure water pervaporation, which is needed for determining several unknown parameters of the model including permeability coefficient, was added. For permeate pressure 5 mm Hg, pervaporation experiments with pure water were not carried out based on the ground that, in line with the "solution-diffusion" concept, permeability coefficient is not dependent on permeate pressure, and it is, indeed, only a function of temperature. Therefore, permeability coefficient can be determined from temperature dependence of pure substance's flux at certain magnitude of the process's driving force. Values of organic component flux $\bar{j}_B$ and total permeate flux $\bar{j}$ are not presented here, as they can be easily obtained from values of water flux $\bar{j}_A$ and separation factor α by carrying out simple calculations.

It can be found from the figure that the curves for calculation results are located rather close to experimental points in the entire range of water concentration in the feed. Use of the model permits expanding results of pervaporation experiments, carried out in the range of water concentration in the feed 0–50 wt%, towards higher concentrations and determining values of water flux for the entire concentration range (0–100 wt%) delivering from the necessity of carrying out additional pervaporation experiments in the range of water concentration in the feed from 50 to 100 wt%.

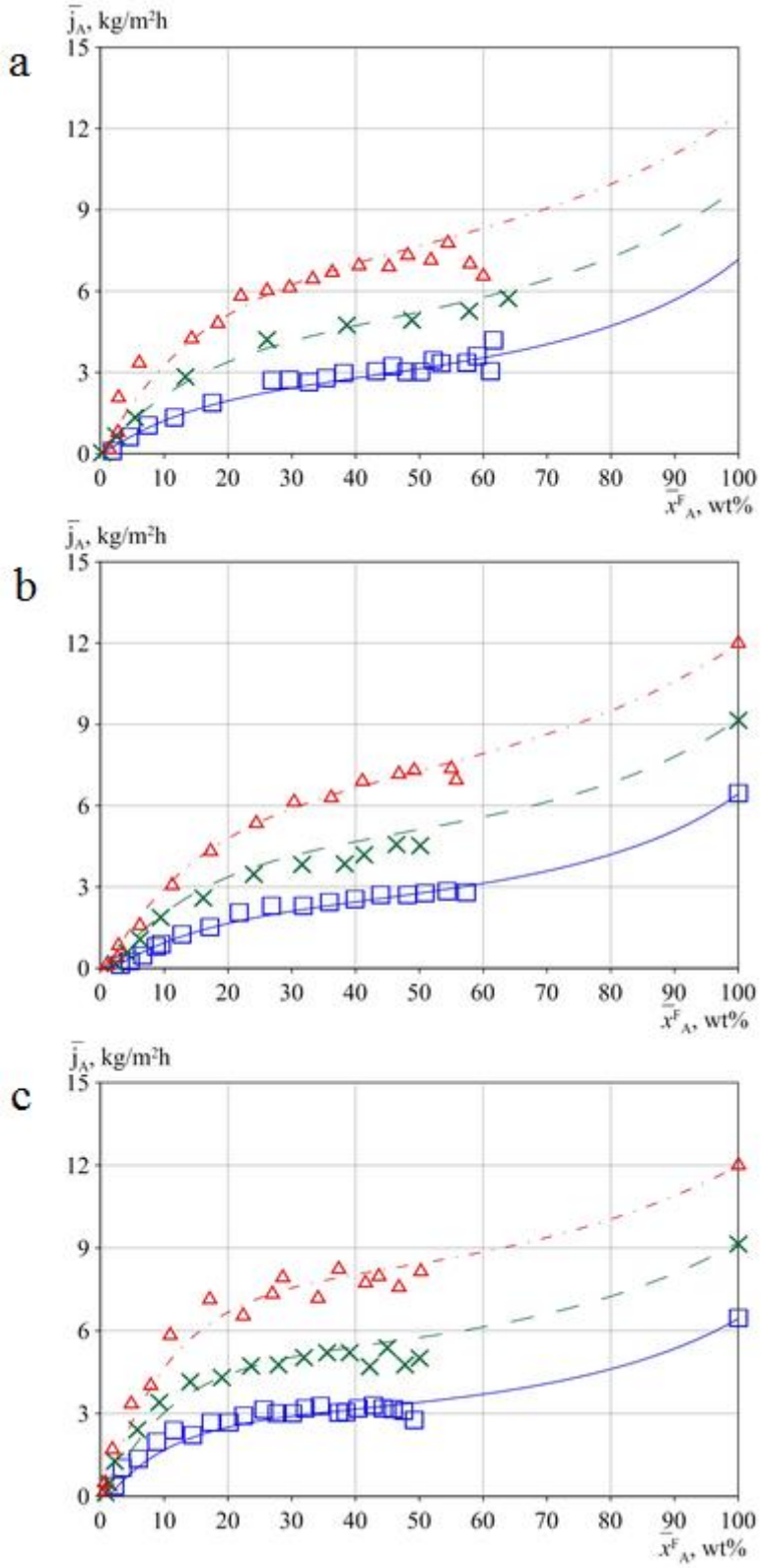

Fig. 7. Dependence of water flux through HybSi membranes on water concentration in the feed at feed temperature 60°C (blue squares – experiments; blue solid line – calculations via the proposed model), 70°C (green crosses – experiments; green dashed line – calculations via the proposed model) and 80°C (red triangles – experiments; red dash-dotted line – calculations via the proposed model). (a) dehydration of ethanol at permeate pressure 5 mm Hg; (b) dehydration of ethanol at permeate pressure 20 mm Hg; (c) dehydration of isopropanol at permeate pressure 20 mm Hg.

4.5. Comparing calculated and measured dependencies of separation factor on water concentration in the feed for dehydrating ethanol and isopropanol by HybSi membranes

Figure 8 presents experimental points and lines corresponding to modeling results for ethanol dehydration at permeate pressure 20 mm Hg and feed temperatures 60, 70 and 80°C. As for the other two cases of alcohol dehydration by HybSi membranes, no comparisons between calculations and experiments are presented here, as coincidence between calculations and experiments was practically very similar.

It can be found from Fig. 8 that both experiments and modeling results exhibit existence of maxima on the curve of dependence of separation factor α on water concentration in the feed $\overline{x}^{F}_{A}$. Calculated magnitudes of maxima of α depart from measured magnitudes by not more than ±20%. In addition, the model predicts accurately concentrations $\overline{x}^{F}_{A}$ corresponding to maxima of α.

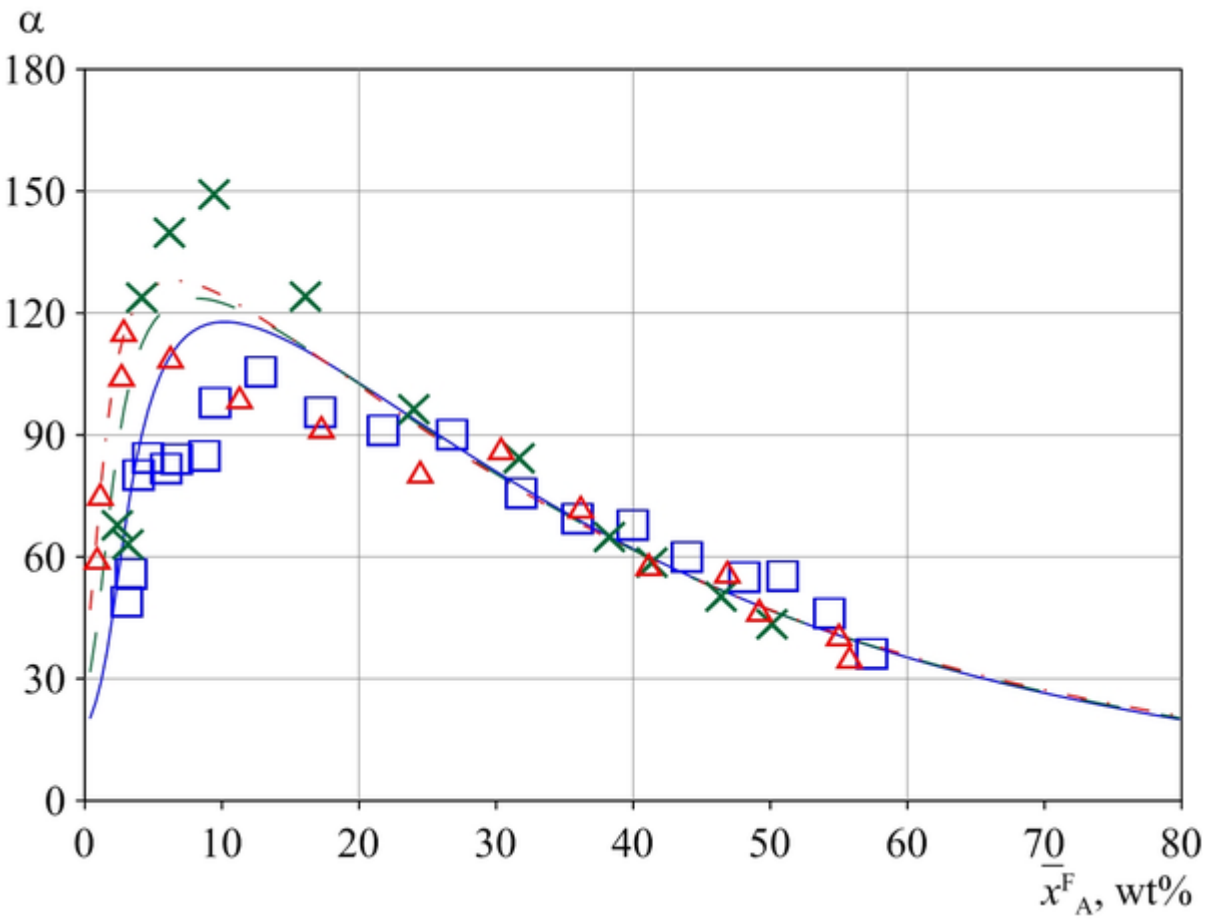

Fig. 8. Dependence of separation factor of HybSi membranes on water concentration in the feed for dehydrating ethanol at permeate pressure 20 mm Hg and feed temperature 60°C (blue squares – experiments; blue solid line – calculations via the proposed model), 70°C (green crosses – experiments; green dashed line – calculations via the proposed model) and 80°C (red triangles – experiments; red dash-dotted line – calculations via the proposed model).

Figure 9 presents modeling results for dependence of separation factor on water flux at permeate pressures in the range from 1 to 200 mm Hg. As it can be found from the figure, calculated dependences have a linear character, and slope angles depend on feed temperature. In addition, the figure presents experimental points. Symbols drawn using dashed lines are "phantom" points indicating positions of experimental points on calculated lines for ideal agreement between experiments and calculations. In view of proximity of calculated lines to experimental points, it can be concluded that the model predicts dependence of separation factor on water flux qualitatively well for cases under consideration.

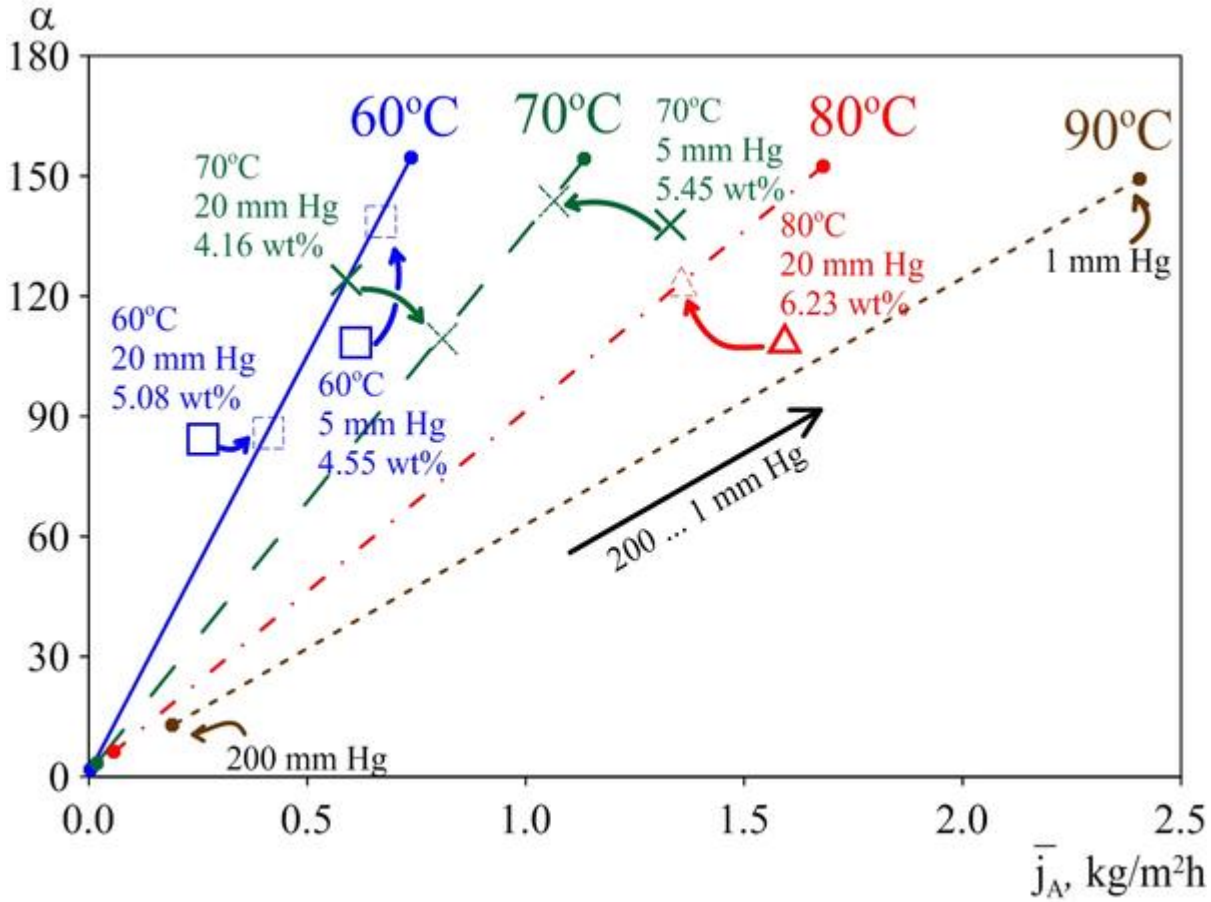

Fig. 9. Calculated and measured dependencies of separation factor on water flux through HybSi membranes for dehydrating ethanol at permeate pressures in the range from 1 to 200 mm Hg and feed temperature 60°C (blue solid line – calculations via the proposed model; blue squares – experiments; blue squares drawn using dashed lines – "phantom" points for the case of ideal coincidence between calculations and experiments), 70°C (green dashed line – calculations via the proposed model; green crosses – experiments; green crosses drawn using dashed lines – "phantom" points for the case of ideal coincidence between calculations and experiments), 80°C (red dash-dotted line – calculations via the proposed model; red triangle – experiments; red triangle drawn using dashed lines – "phantom" point for the case of ideal coincidence between calculations and experiments) and 90°C (brown line made of short dashes – calculations via the proposed model).

4.6. Comparing calculated and measured dependences of water flux on water concentration in the feed obtained in the present study with data of other researchers

The model was also used to obtain curves for dependence of water flux on water concentration in the feed for other binary water/organic mixtures and pervaporation membranes from the literature. Figure 10 presents experimental data for dehydration of ethanol by NaA

zeolite membranes from [19] and dehydration of glycerin by HybSi membranes from [4] together with our own data obtained in the present study for dehydration of ethanol and isopropanol by HybSi membranes.

As it can be found from Fig. 10, water flux through HybSi membranes is greater for isopropanol/water mixture dehydration than for ethanol/water mixture dehydration. On the other hand, when HybSi membranes are used, organic component flux for isopropanol dehydration is smaller by one order of magnitude than that for ethanol dehydration (see Fig. 5), and for glycerin dehydration, organic component flux is practically zero [4]. It can be assumed that differences in permeation of organic component through HybSi membranes are related to differences in sizes of molecules of ethanol, isopropanol and glycerin, which leads to differences in diffusion of substances through the membranes (an ethanol molecule is smaller than an isopropanol molecule, which, in turn, is smaller than a glycerin molecule). In addition, if relative volatility of water in the considered binary mixtures is considered, then relative volatility is found to increase in the order: ethanol/water, isopropanol/water and glycerin/water, which is a supplementary explanation for the observation about permeation of the three organic substances through the membranes. On the other hand, glycerin is a triatomic alcohol and a glycerin molecule contains three hydroxyl groups (–OH) in place of one as in monoatomic alcohols: ethanol or isopropanol. This characteristics promotes hydrogen binding of glycerin molecules inside HybSi's pores by means of hydroxyl groups, which makes it impossible for glycerin molecules passing through HybSi membranes. A similar explanation was provided in [30] and [6] for nearly infinite selectivity of titania and hybrid silica membranes, respectively, for deep dehydration of ethylene glycol and diethylene glycol, respectively (both organic substances are diatomic alcohols). Hydrogen binding might also be a good explanation for almost complete impermeability of HybSi membranes to glycerin.

As it can be found from Fig. 10, calculated curves diverge from experimental points insignificantly. Values of determination coefficient R^2 are equal to 0.9412, 0.9441, 0.9879 and 0.9920 for cases of dehydration of ethanol/water (HybSi), isopropanol/water (HybSi), glycerin/water (HybSi) and ethanol/water (NaA-zeolite), respectively. Thus, it can be concluded regarding applicability of the developed model for these membranes and binary mixtures. In calculating R^2 for glycerin/water (HybSi) case, only the first two (on the left) experimental points were used. For obtaining a curve, passing rather closely to the remaining two (on the right) experimental points, the Langmuir adsorption isotherm must be replaced with a more complex adsorption isotherm.

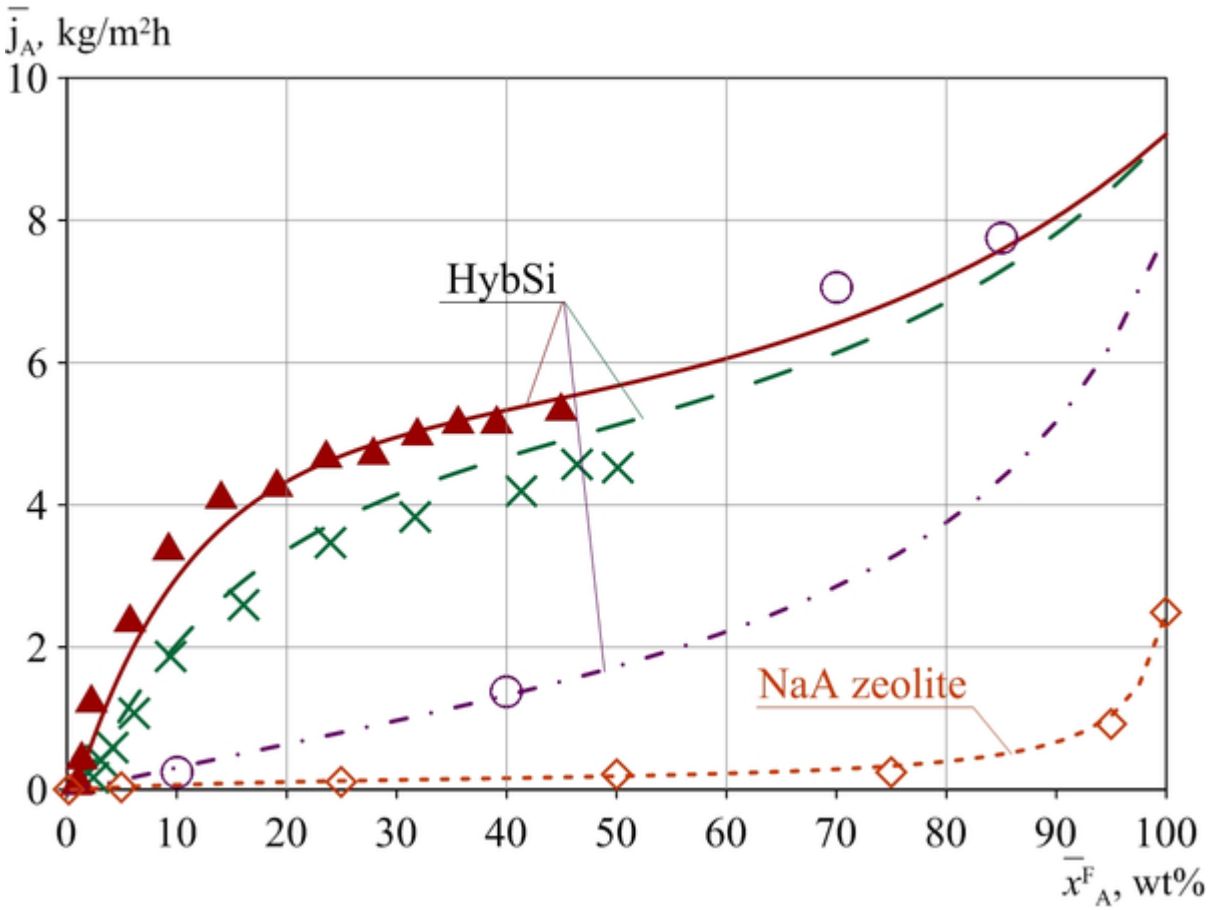

Fig. 10. Dependence of water flux on water concentration in the feed for various mixtures and membranes: ▲ – dehydration of isopropanol by HybSi membranes at feed temperature 70°C and permeate pressure 20 mm Hg (present study); × – dehydration of isopropanol by HybSi membranes at feed temperature 70°C and permeate pressure 20 mm Hg (present study); ○ – dehydration of glycerin by HybSi membranes at feed temperature 65°C and permeate pressure 7.5 mm Hg [4]; ◊ – dehydration of ethanol by NaA-zeolite membranes at feed temperature 70°C and permeate pressure 1 mm Hg [19]. Lines – results of calculations via the proposed model for identical process conditions.

All curves for calculation results were obtained at value of active pores fraction $\varepsilon_a<1$, which implies that during diffusive mass transfer through membranes, only a fraction of pores, called as "active", is used for mass transfer. This assumption is critical for modeling pervaporation through dense (non-porous) membranes. If all pores were assumed to be open and active, $\varepsilon_a=1$, then, for glycerin/water (HybSi) case, driving force for pervaporation through HybSi membranes would be greatest and exceed driving force for pervaporation of ethanol/water (HybSi) and isopropanol/water (HybSi) mixtures. However, as it can be found from Fig. 10, water flux for ethanol/water (HybSi) and isopropanol/water (HybSi) cases exceeds that for glycerin/water (HybSi) case. Thus, the above assumption that component fluxes are influenced not only by a difference in values of permeating component's partial pressure on the two membrane boundaries, but also by active pores fraction, is proven to be valid. It is worth noting that active pores fraction is dependent on feed composition. In the literature, to our best knowledge, no parameter coinciding with "active pores fraction" and bearing the same meaning has ever been introduced up to now. Our modeling results demonstrate that influence of active pores fraction on pervaporation increases with increase in ability of components of two-component feed mixture to permeate through the membranes.

4.7. Calculated dependencies of water flux and separation factor on the selective layer's thickness of HybSi membranes, reduced mass transfer coefficient and water concentration in the feed

Figure 11 presents calculated dependencies of water flux and separation factor on selective layer's thickness of HybSi membranes in the range 0–100 nm for ethanol/water mixture dehydration at feed temperature 60°C and permeate pressure 5 mm Hg at values of water concentration in the feed 5, 20 and 80 wt%. As is seen from the figure, with increase of selective layer's thickness, separation factor grows, at first, and reaches a constant (weakly varying) value afterwards. At the same time, water flux decreases monotonically. From the data it be concluded that optimum thickness of HybSi membrane's selective layer is on the order of ~50 nm, which is technically achievable, when the sol-gel method is used.

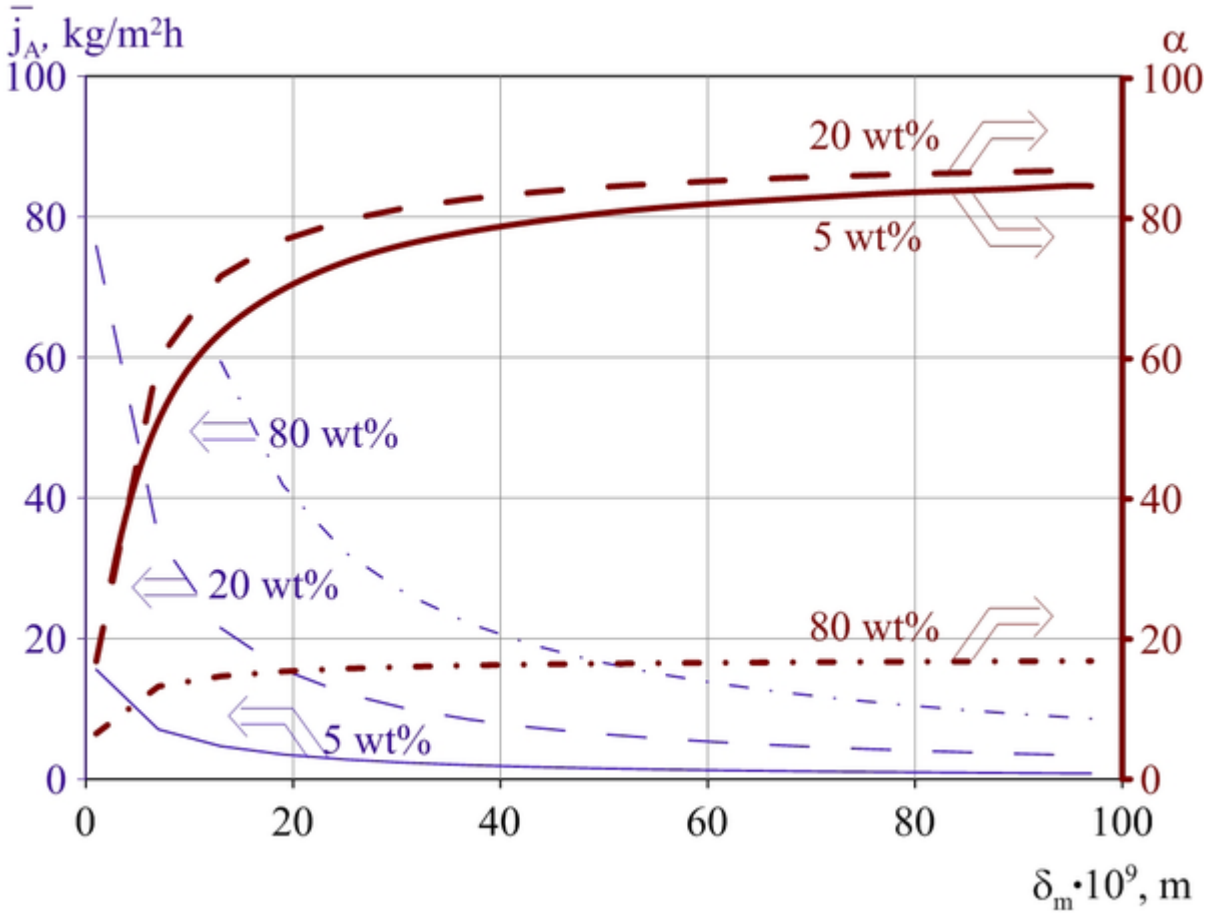

Fig. 11. Calculated dependencies of water flux and separation factor on the selective layer's thickness of HybSi membranes at dehydration of ethanol/water mixture at feed temperature 60°C and permeate pressure 5 mm Hg: solid line – concentration of water in the feed 5 wt%; dashed line – concentration of water in the feed 20 wt%; dash-dotted line – concentration of water in the feed 80 wt%.

Figure 12 presents calculated dependences of water flux and separation factor on reduced mass transfer coefficient β^*, [m/s], defined as mass transfer coefficient multiplied by the mixture's molecular weight and divided by the mixture's mass density. Limiting stages of mass transfer from the feed stream to the permeate zone are easily distinguishable. For example, when β* drops below 0.4, considerable reduction of water flux and separation factor is observed. Apparently, for β^* values within this range, limiting stage of mass transfer is transport of mixture components from the liquid phase's flow core to the membrane surface. As β^* increases above 0.4, limiting stage of mass transfer is gradually shifted towards transport of mixture components through the membrane. Thus, data of Fig. 12 allow determining reduced mass transfer coefficient

β^* and average velocity of feed mixture in the membrane module w_{lin}, corresponding to β^*, above which there exists no observable increase in water flux and separation factor.

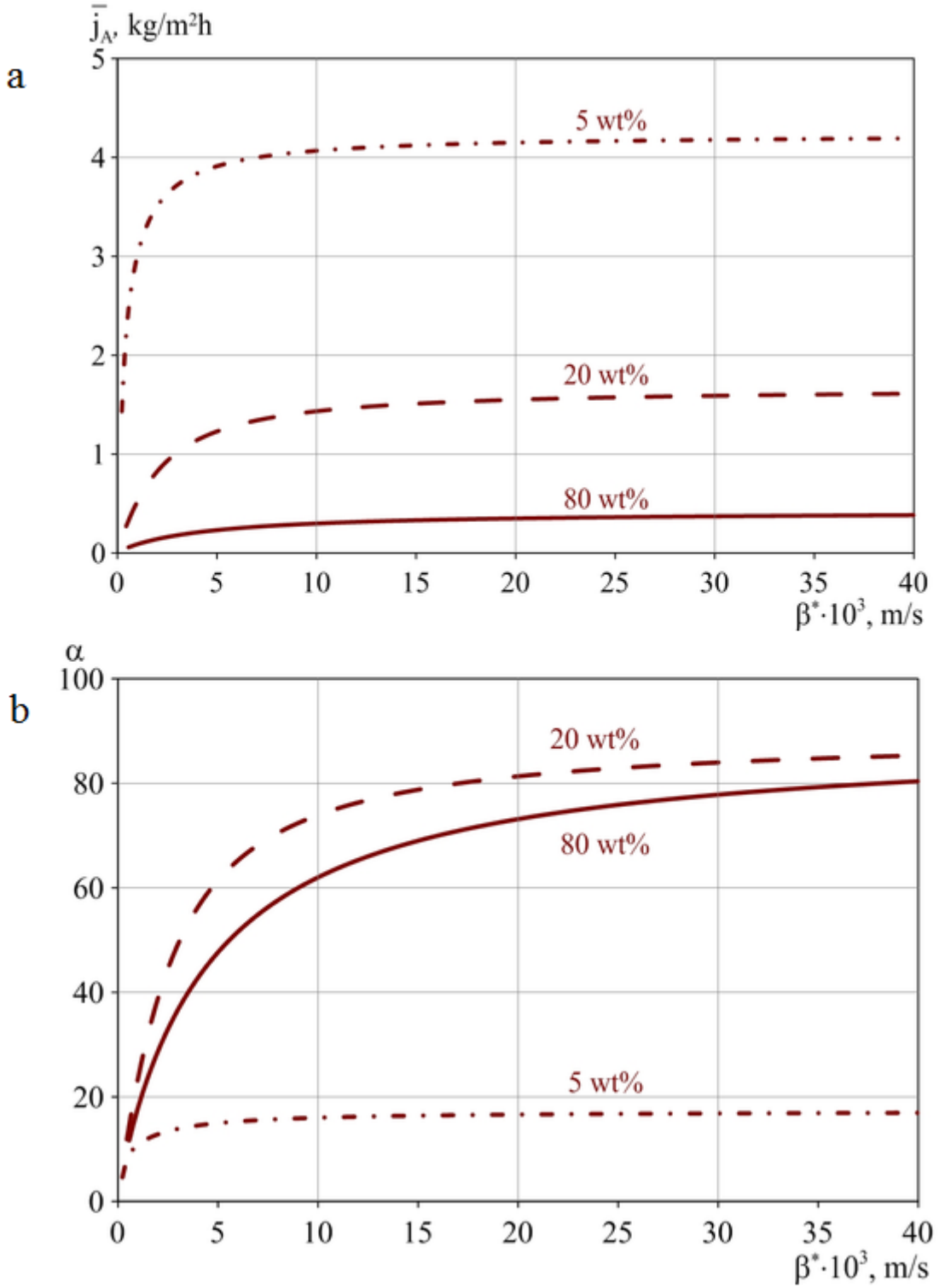

Fig. 12. Calculated dependencies of water flux and separation factor on reduced mass transfer coefficient β^* for dehydration of ethanol/water mixture by HybSi membranes at feed temperature 60°C and permeate pressure 20 mm Hg:
solid line – concentration of water in the feed 5 wt%;
dashed line – concentration of water in the feed 20 wt%;
dash-dotted line – concentration of water in the feed 80 wt%.
(a) water flux;
(b) separation factor.

Figure 13 presents calculated dependencies of separation factor of HybSi membranes on water concentration in the feed for dehydration of ethanol and isopropanol. It can be found that under identical process conditions and feed compositions, separation factor for isopropanol dehydration is greater than that for ethanol dehydration by approximately two orders of magnitude. In all three cases, with decrease in water concentration in the feed, separation factor grows, at first, until reaching a maximum value, and drops afterwards.

At dehydrating ethanol at feed temperature 70°C, a maximum value of separation factor is observed at water concentration in the feed ~10 wt%, when permeate pressure is 20 mm Hg. When permeate pressure is reduced to 5 mm Hg, water concentration in the feed, corresponding to a maximum value of separation factor, is shifted towards 5 wt%. At feed temperatures 60 and 80°C, similar shiftings are observed, when permeate pressure is reduced from 20 to 5 mm Hg. Existence of a maximum in all three cases can be explained with the fact that at certain water concentration in the feed, water flux significantly decreases due to depletion of water component on the feed side of the unit during dehydration, and organic component flux remains practically unchanged or even increases slightly. Existence of a maximum on the curves must be taken into account during selecting the most optimal process conditions for a pervaporation pilot plant equipped with HybSi membranes.

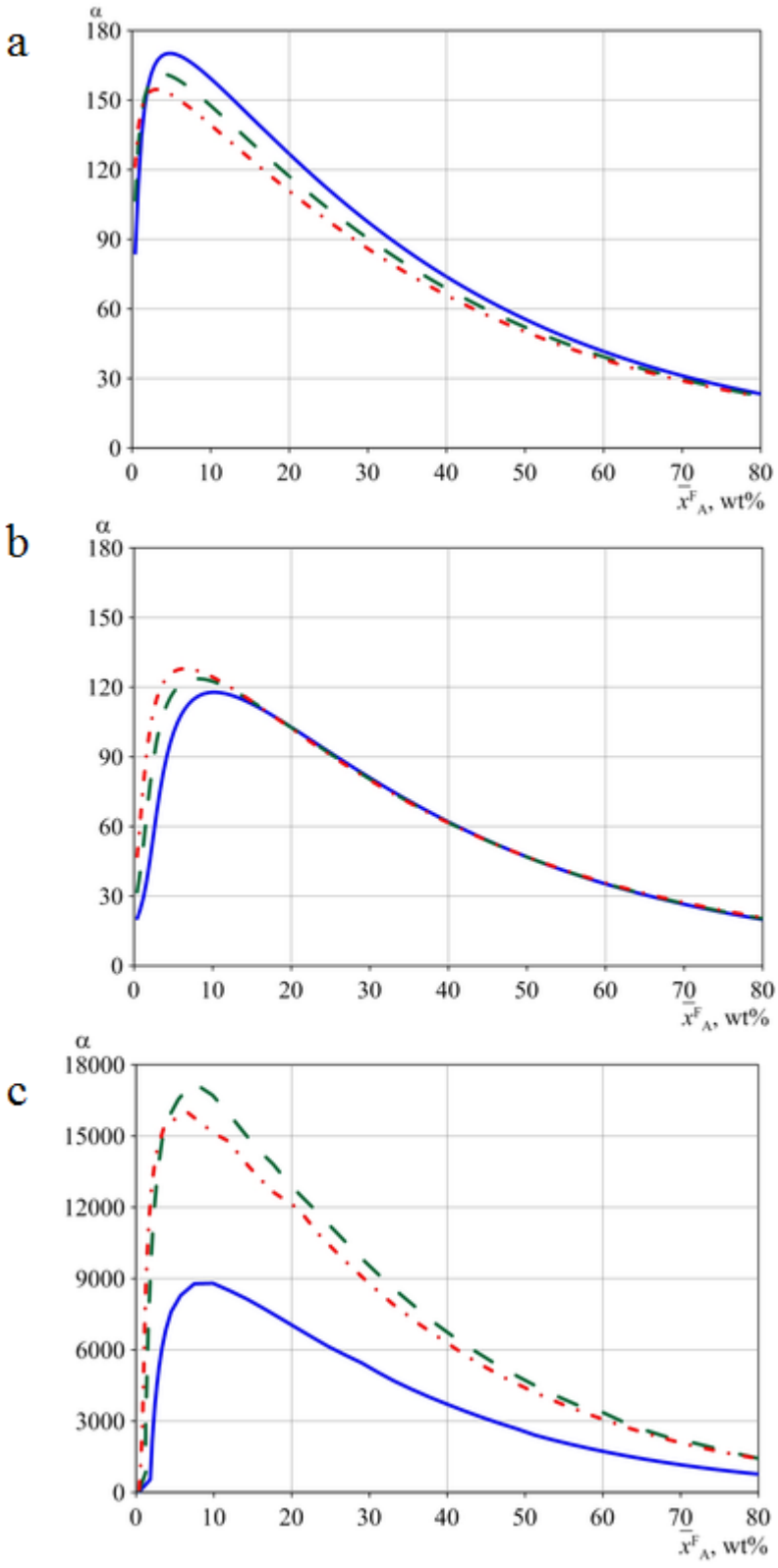

Fig. 13. Dependence of modeled separation factor on water concentration in the feed at feed temperature 60°C (blue solid line), 70°C (green dashed line) and 80°C (red dash-dotted line) for dehydration by HybSi membranes. (a) dehydration of ethanol at permeate pressure 5 mm Hg; (b) dehydration of ethanol at permeate pressure 20 mm Hg; (c) dehydration of isopropanol at permeate pressure 20 mm Hg.

4.8. Calculated dependencies of active pores fraction on process parameters at ethanol dehydration by HybSi membranes

Figures 14 and 15 present calculated dependencies of active pores fraction on water concentration in the feed and feed temperature at dehydration of ethanol/water mixture at permeate pressure 20 mm Hg. As is seen from the figures, active pores fraction increases with increase of feed temperature, which points to reduction of quantity of adsorbed molecules on the HybSi membrane surfaces as well as on the channels. Therefore, for increasing efficiency of pervaporation through HybSi membranes, feed temperature must be lifted up to some higher values. As it was indicated in our previous study (Akberov et al., 2015), the optimum range of operating temperatures for HybSi membranes is shifted towards higher temperature values in comparison with polymeric membranes.

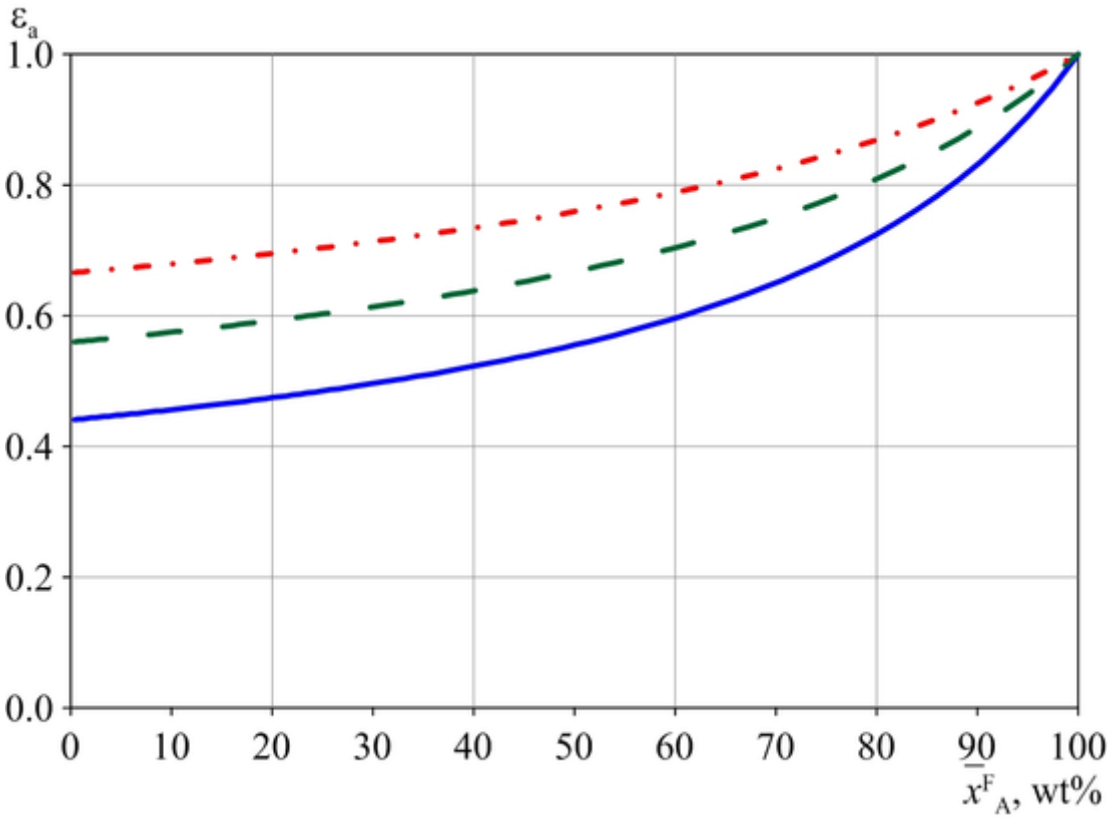

Fig. 14. Calculated dependencies of active pores fraction on water concentration in the feed at dehydration of ethanol/water mixture at permeate pressure 20 mm Hg and feed temperature 60°C (blue solid line), 70°C (green dashed line) and 80°C (red dash-dotted line).

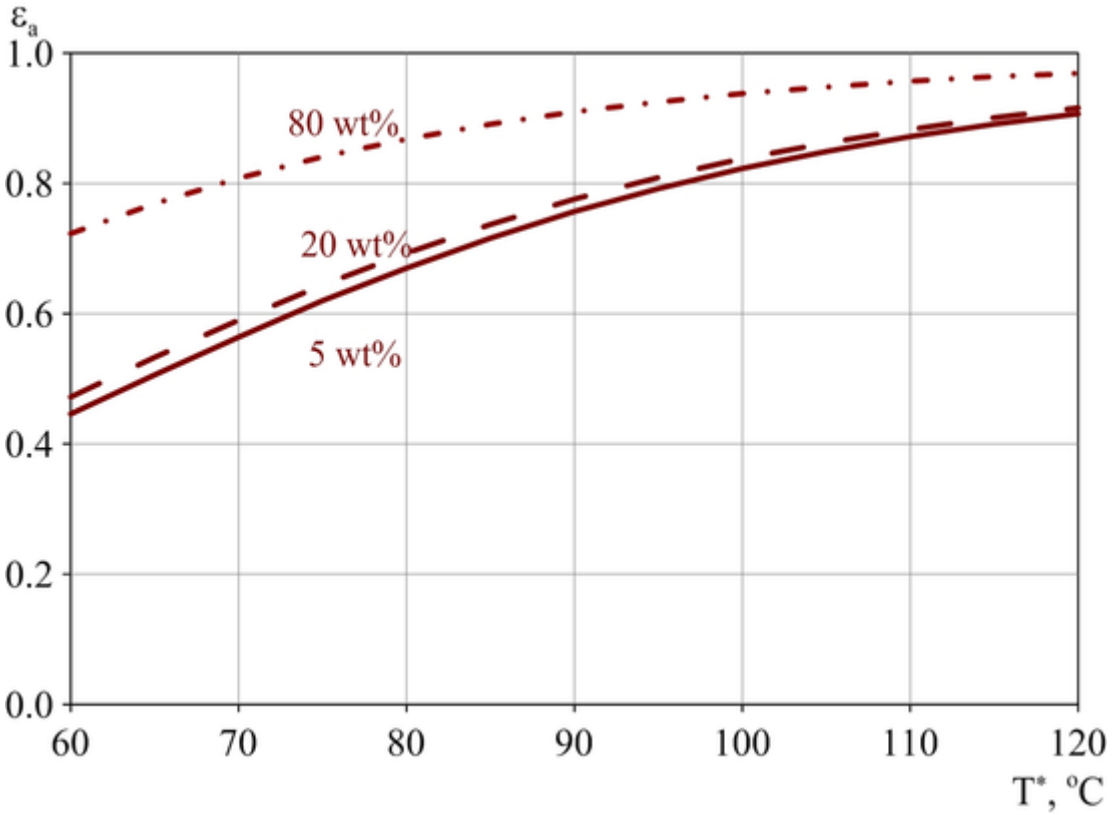

Fig. 15. Calculated dependencies of active pores fraction on feed temperature at dehydration of ethanol/water mixture at permeate pressure 20 mm Hg and water concentration in the feed 5 wt% (solid line), 20 wt% (dashed line) and 80 wt% (dash-dotted line).

5. Conclusions

Carried out experimental investigation using ceramic membranes HybSi allows drawing the following conclusions. Values of separation factor and total permeate flux turn out to be higher for isopropanol dehydration than for ethanol dehydration. For ethanol dehydration, when water concentration in the feed drops below 10–20 wt%, ethanol concentration in permeate increases sharply; the problem does not appear during isopropanol dehydration. The difference in permeation of organic component through HybSi membranes can be explained by difference in diffusion of organic component through the membranes related to differences in sizes of molecules of ethanol and isopropanol as well as by difference in relative volatility of water in ethanol/water and isopropanol/water mixtures. In addition, the experiments have shown that dependence of separation factor on water concentration in the feed is nonmonotonic; the maximum value of separation factor is reached at concentration of water in the feed of several percent. This should be taken into account during selecting optimum operating conditions of a pervaporation plant.

From analysis of calculation results obtained via the proposed model, the following conclusions can be drawn. The model is capable of correctly reproducing a measured maximum value of separation factor on the curve of dependence of separation factor on water concentration in the feed. In addition, the model reproduces correctly dependence of water flux on water concentration in the feed in the entire concentration region at dehydration of ethanol and isopropanol by HybSi membranes as well at dehydration of ethanol by NaA zeolite membranes (experimental data of other researchers). As for glycerin dehydration by HybSi membranes (experimental data of other researchers), significant divergence between calculations and experiments is observed for water concentrations in the feed above 60 wt% implying a need of replacement of the Langmuir adsorption isotherm with a more complex adsorption isotherm. Calculation results indicate that optimum thickness of selective layer of HybSi membranes is on

the order of ~50 nm. A parameter of the model introduced under the name “active pores fraction” was less than 1 for all considered cases. Hence, during pervaporation the mass transfer through considered HybSi and NaA zeolite membranes occurs only through “active” pores or channels on the surface of the selective layer of the membranes. Results of conducted investigation show that both water flux and organic component flux increase linearly with increase in feed temperature.

Conducted investigation demonstrates potential applicability of ceramic membranes HybSi for creating pervaporation pilot plants destined for separation of ethanol/water and isopropanol/water mixtures as well as applicability of the developed approach of modeling the pervaporation process using the “solution-diffusion” and “active pores fraction” concepts for predicting separation characteristics of pervaporation membranes (in particular, HybSi and NaA zeolite membranes), when a limited amount of experimental data is available, and for developing membranes with predefined values of total permeate flux and separation factor. Results of investigation can be used for designing pervaporation pilot plants and developing various theoretical (perhaps, even more advanced) models of separation.

Acknowledgments

The work was partly funded in accordance with the Russian Government Program of Competitive Growth of Kazan Federal University.

References

[1] A. Jonquières, R. Clément, P. Lochon, J. Néel, M. Dresch, B. Chrétien, Industrial state-of-the-art of pervaporation and vapour permeation in the western countries, J. Membr. Sci. 206 (2002) 87–117.

[2] H.L. Castricum, R. Kreiter, H.M. van Veen, D.H.A. Blank, J.F. Vente, J.E. ten Elshof, High-performance hybrid pervaporation membranes with superior hydrothermal and acid-stability, J. Membr. Sci. 324 (2008) 111–118.

[3] H.M. van Veen, M.D.A. Rietkerk, D.P. Shanahan, M.M.A. van Tuel, R. Kreiter, H.L. Castricum, J.E. ten Elshof, J.F. Vente, Pushing membrane stability boundaries with HybSi® pervaporation membranes, J. Membr. Sci. 380 (2011) 124–131.

[4] S.-K. Mah, S.-P. Chai, T.Y. Wu, Dehydration of glycerin solution using pervaporation: HybSi and polydimethylsiloxane membranes, J. Membr. Sci. 450 (2014) 440–446.

[5] R.R. Akberov, A.R. Fazlyev, A.V. Klinov, A.V. Malygin, M.I. Farakhov, V.A. Maryakhina, S.M. Kirichenko, Dehydration of diethylene glycol by pervaporation using HybSi ceramic membranes, Theor. Found. Chem. Eng. 48 (2014) 650–655.

[6] R.R. Akberov, A.R. Fazlyev, A.V. Klinov, A.V. Malygin, M.I. Farakhov, V.A. Maryakhina, Pervaporation technology for regeneration of diethylene glycol at Russian complex gas treatment plants with the use of ceramic membranes HybSi, J. Nat. Gas Sci. Eng. 26 (2015) 670–682.

[7] T. Graham, On the absorption and dialytic separation of gases by colloid septa, Phil. Trans. 156 (1866) 399–439.

[8] L.Y. Jiang, Y. Wang, T.S. Chung, X.Y. Qiao, J.Y. Lai, Polyimides membranes for pervaporation and biofuels separation, Prog. Polym. Sci. 34 (2009) 1135–1160.

[9] Y. Wang, S.H. Goh, T.S. Chung, N. Peng, Polyamide-imide/polyetherimide dual-layer hollow fiber membranes for pervaporation dehydration of C1-C4 alcohols, J. Membr. Sci. 326 (2009) 222–233.

[10] J.G. Wijmans, R.W. Baker, The solution-diffusion model: a review, J. Membr. Sci. 107 (1995) 1–21.

[11] X. Feng, R.Y.M. Huang, Liquid separation by membrane pervaporation: a review, Ind. Eng. Chem. Res. 36 (1997) 1048–1066.

[12] W.F. Guo, T.S. Chung, T. Matsuura, Pervaporation study on the dehydration of aqueous butanol solutions: a comparison of flux vs. permeance, separation factor vs. selectivity, J. Membr. Sci. 245 (2004) 199–210.

[13] X.Y. Qiao, T.S. Chung, W.F. Guo, T. Matsuura, M.M. Teoh, Dehydration of isopropanol and its comparison with dehydration of butanol isomers from thermodynamic and molecular aspects, J. Membr. Sci. 252 (2005) 37–49.

[14] Y. Wang, L.Y. Jiang, T. Matsuura, T.S. Chung, S.H. Goh, Investigation of the fundamental differences between polyamide-imide (PAI) and polyetherimide (PEI) membranes for isopropanol dehydration via pervaporation, J. Membr. Sci. 318 (2008) 217–226.

[15] L.Y. Jiang, T.S. Chung, Homogeneous polyimide/cyclodextrin composite membranes for pervaporation dehydration of isopropanol, J. Membr. Sci. 346 (2010) 45–58.

[16] Y. Wang, T.S. Chung, B. Neo, M. Gruender, Processing and engineering of pervaporation dehydration of ethylene glycol via dual-layer polybenzimidazole (PBI)/polyetherimide (PEI) membranes, J. Membr. Sci. 378 (2011) 339–350.

[17] N.L. Le, Y. Wang, T.S. Chung, Poly(ether-block-amide)/POSS mixed matrix membranes for ethanol recovery from aqueous solutions, J. Membr. Sci. 379 (2011) 174–183.

[18] G.M. Shi, Y. Wang, T.S. Chung, Dual-layer PBI/P84 hollow fibers for pervaporation dehydration of acetone, AIChE J. 58 (2012) 1133–1145.

[19] C.H. Cho, K.Y. Oh, J.G. Yeo, S.K. Kim, Y.M. Lee, Synthesis, ethanol dehydration and thermal stability of NaA zeolite/alumina composite membranes with narrow non-zeolitic pores and thin intermediate layer, J. Membr. Sci. 364 (2010) 138–148.

[20] A.I. Razinov, O.V. Maminov, G.S. Dyakonov, Theoretical Foundations of Chemical Engineering Processes, Kazan State Technological University Press, Kazan, 2005.

[21] R.W. Baker, Membrane Technology and Applications, second ed., John Wiley and Sons Inc., Chichester, 2004.

[22] H. Renon, J.M. Prausnitz, Local compositions in thermodynamic excess functions for liquid mixtures, AIChE J. 14 (1968) 135–144.

[23] A.G. Kasatkin, Basic Processes and Apparatuses in Chemical Technology, OOO TID “Alliance”, Moscow, 2005.

[24] H.M. van Veen, Y.C. van Delft, C.W.R. Engelen, P.P.A.C. Pex, Dewatering of organics by pervaporation with silica membranes, Sep. Purif. Technol. 22–23 (2001) 361–366.

[25] R.W. van Gemert, F.P. Cuperus, Newly developed ceramic membranes for dehydration and separation of organic mixtures by pervaporation, J. Membr. Sci. 105 (1995) 287–291.

[26] M. Kondo, M. Komori, H. Kita, K. Okamoto, Tubular-type pervaporation module with zeolite NaA membrane, J. Membr. Sci. 133 (1997) 133–141.

[27] A. Urtiaga, C. Casado, M. Asaeda, I. Ortiz, Comparison of SiO2-ZrO2-50% and commercial SiO2 membranes on the pervaporative dehydration of organic solvents, Desalination 193 (2006) 97–102.

[28] A.W. Verkerk, P. van Male, M.A.G. Vorstman, J.T.F. Keurentjes, Properties of high flux ceramic pervaporation membranes for dehydration of alcohol/water mixtures, Sep. Purif. Technol. 22–23 (2001) 689–695.

[29] J.J. Jafar, P.M. Budd, Separation of alcohol/water mixtures by pervaporation through zeolite A membranes, Microporous Mater. 12 (1997) 305–311.

[30] J. Sekulic, J.E. ten Elshof, D.H.A. Blank, Selective pervaporation of water through a nonselective microporous titania membrane by a dynamically induced molecular sieving mechanism, Langmuir 21 (2005) 508–510.